

Authors' Answers to the Referees' Comments

The authors thank the referees for their useful comments and suggestions to improve the clarity and readability of the paper. In the following we reply to their comments:

Referee #1

General Comment :

The authors should make a stronger case earlier in the article.

Reply:

We added a sentence on page 7242, line 11 to indicate that we plan to use the new formalism to obtain the quantum yields for the isotopologue CHDO.

General Comment :

I suggest the authors include both the 2006 and 2013 IUPAC recommendations.

Reply:

The 2013 IUPAC recommendations are included in all relevant figures and in the discussion.

General Comment :

There is a degree of redundancy. Some consolidation would be helpful.

Reply:

All tables except Table 4 are omitted and the 1σ errors included in the respective equations.

Specific Comment p.7242, l.5 :

Express as summation, with the A parameter a signed quantity?

Reply:

On page 7242, line 4 we replaced 'combination' by 'sums'. This should make clear what is meant.

Specific Comment p.7242, l.13 :

The criteria for rejecting some measurements are unclear

Reply:

We changed that sentence by specifying the criteria for rejecting measurements. We also listed explicitly the measurements not included.

Specific Comment p.7243, l.121 :

typo – ‘wavelength’

Reply:

corrected

Specific Comments p.7243, l.26 and p.7247, l.13 :

‘heat of formation’ should be ‘heat of reaction’

Reply:

changed

Specific Comment p.7242, l.5 :

Invoking a threshold for three-body dissociation does not help to explain the apparent decrease in the photolysis quantum yield.

Reply:

We agree, nevertheless we find the coincidence interesting.

Specific Comment p.7248, l.6 :

Equation (7) seems superfluous.

Reply:

We agree and omitted the equation.

Specific Comment p.7250, l.9 :

Replace ‘frequencies’ with ‘rates’.

Reply:

The term ‘photolysis frequency’ is generally used in our field. For consistency we prefer to keep it here, too.

Specific Comment p.7251, l.5 :

Equations 11 – 13 do not appear in the manuscript.

Reply:

The Table 1 (formerly Tab.4) with these equations (now numbered 8 to 10) is included in the text in due place.

Specific Comment p.7251, l.15-25 :

- (1) The effect of the temperature dependence of the absorption cross section should be addressed.
- (2) The variations of -9% and +6% in j_{rad} and j_{mol} are described as a significant effect. This seems inconsistent with the comment on page 7244, line 19-24. Why is -4% small, but +6% significant?

Reply:

- (1) Its effect on the j_i is small, less than 0.3 % for j_{rad} and less than 3% for j_{tot} and included in the calculation. We added a sentence (page.7250, line15) to indicate the size of the effect.
- (2) To resolve the apparent inconsistency we have changed the text on page 7244, line23 to indicate that the superposition of the line at 321 nm from Tatum Ernest et al. (2012) on our Φ_{rad} , Eq.(3), would cause an increase in j_{mol} by less than 2 % at all altitudes and a decrease in j_{rad} by less than 4 %. These upper limits are more than a factor of 2 smaller than the changes of +6 % and - 9 % for j_{mol} and j_{rad} at 15 km altitude due to the assumed temperature dependence of Φ_{rad} .

Specific Comment p.7262 :

typo 'Gratien' in figure caption

Reply:

corrected.

Referee #2

General Comment :

The discussion of the quantum yield temperature dependence and its impact on atmospheric photolysis rates seems out of place.

Reply:

The idea is to show the impact of a possible temperature dependence of Φ_{rad} on j_{rad} and j_{mol} to see whether that effect is significant and needs further attention.

Comment p.7264, Figure 4 :

It would be very instructive to include an additional panel that shows the wavelength dependence of the product of the terms shown in this figure.

Reply:

The product is included.

Technical Comment p.7240, l.1:

delete 'various'

Reply:

deleted

Technical Comment p.7240, equations :

It would be useful to provide the photolysis threshold wavelengths (energies) along with the possible photolysis channels.

Reply:

We prefer to introduce the photolysis thresholds in the respective section where they are needed.

Technical Comment p.7241 :

Fluorescence is noted here to account for a small yield in the photolysis of CH₂O. I suggest the authors reconsider their decision to neglect fluorescence even if only a minor term.

Reply:

Given the experimental uncertainties in the Φ_i which are on the order of 10 %, our formalism does not include effects which amount to a few % corrections, such as the line structure in Φ_{rad} by Tatum Ernest et al. (2012) or here the fluorescence. But they are mentioned in the text to inform the reader.

Technical Comment p.7242, l.3: :

'a more handy tool ...': The proposed parametrization is more physically based, but not necessarily easier to implement.

Reply:

We changed the sentence on line 2 to make clear that the fourth order polynomial exists only for Φ_{rad} . We are of the opinion that the fit by a functional term is more handy than a look-up table.

Technical Comment p.7243, l.5 :

delete 'without any weighing'

Reply:

deleted

Technical Comment p.7243, l.12 :

wavelengths

Reply:

corrected

Technical Comment p.7244, l.9 :

delete 'Discussion'

Reply:

deleted

Technical Comment p.7246, l.1 :

'vanishes' poor wording

Reply:

We prefer to keep 'vanishes'

Technical Comment p.7249 :

equations 11 – 13 do not exist in the paper

Reply:

The Table 1 (formerly Tab.4) with these equations (now numbered 8 to 10) is included in the text in due place.

Referee #3

Comment p.7242, l.12-16 and p.7243,l.3-14

The authors should discuss in more detail their selection criteria and should incorporate the recent high structured QY data of Tatum Ernest et al. (2012) in their analysis.

Reply:

We changed that sentence on page7242, line13 by specifying the criteria for rejecting measurements. We also listed explicitly the measurements not included. We also

added a sentence on page7242, line23 that quantify the effect of a superposition of the line at 321 nm from Tatum Ernest et al. on our Eq.(3) for Φ_{rad} on the photolysis rates in the atmosphere. (see reply to Referee #1)

Comment p.7243,l. 10-17 and Fi.1 to 3

- (1) It is not clear from the text if the fit shown in Fig.1 represents Eq.(3) or Eq.(11) of Table 4.
- (2) Is it possible to improve the fitting at the plateau and tail of the QY curve of Fig.1 ?

Reply:

- (1) The respective equations are now added to the legends.
- (2) As we discussed in the text on page7244, line17, there is the possibility to improve the fitting by a wavelength-dependent parameter b, once sufficiently accurate data become available. Another possibility was applied by Troe (2007) who multiplied the QY by a function of the type of Eq.(2). If the tail is cut off at 340 nm, the photolysis frequency is diminished by less than 10 % at all altitudes.

Comment p.7245, l.10

What is the correlation coefficient for IUPAC 2013 ?

Reply:

The coefficient of determination is added to the text, its value is 0.876.

Comment p.7248, l.6-11

It would be interesting to graphically compare the QY curves obtained by the individual Eqs.(3), (4), and (6) with the QY curves obtained by the simultaneous fit of Eqs. (11)-(13). Moreover it would be advantageous to list the recommended QY from Eqs. (11) to (13) in tabular form.

Reply:

We prefer to keep the figures as they are, further addition of curves would make them rather busy.

Comment p.7250, l.14

Preferably another reference should be used for Gratien et al. (2007)

Reply:

We changed the reference.

Comment p.7251, l.5

What is the resolution of the formaldehyde absorption cross section used? Have the authors considered using other available absorption spectra at higher resolution?

Reply:

All calculations were carried out with a resolution of 1 nm, as now mentioned in the text on page 7251, line 17. To check the influence of the absorption cross section's resolution we used the high resolution formaldehyde spectrum of Meller and Moortgat (2000) with a resolution of 0.01 nm. First, we calculated the photolysis frequencies with original spectrum and then with the cross sections integrated over 1 nm. The differences in the j_i are less than 0.1 %, i.e. in the range of the numerical errors.

Comment p.7252, l.9-24 and Fig.6

It would be useful to include the calculation of the j values in Fig.6 using the QY data of IUPAC 2013.

Reply:

These calculations are added in the text and in Fig.6.

Typos and Corrections

Reply:

Typos are corrected.

1 **List of Relevant Changes**

2 A simple formulation of the CH₂O photolysis quantum yields

3 E.-P. Röth¹ and D. H. Ehhalt²

4

5 The following changes were made in the text (referring to the marked-up manuscript) :

6

7 page 2 / line 25

8 For Φ_{rad} also a fit by a fourth order polynomial (see Sander et al., 2011) exists. To provide a

9 more handy tool for atmospheric modeling we propose to use sums of energy dependent

10 functions of the type

$$11 \quad \frac{A}{1+\exp\left[\frac{-(1/\lambda-1/\lambda_0)}{b}\right]} \quad (2)$$

12 to fit Φ_{mol} and Φ_{rad} .

13

14 page 3 / line 1

15 In particular we hope to eventually construct expressions of the quantum yields for CHDO for

16 which –apart from the threshold energies and a few isotope fractionation factors- no direct

17 measurements exist.

18

19 page 3 / line 4 - 13

20 Our analysis of the quantum yields will be based on the data filed by JPL (Sander et al., 2011)

21 and IUPAC (2006) omitting all measurements whose wavelength dependencies deviate

22 strongly from the forms recommended by JPL or IUPAC (e.g. McQuigg and Calvert, Clark et

23 al., Tang et al. for Φ_{rad}). Likewise, if measured data appear in several publications by the same

24 authors, only the latest data were considered. Not all data are independent of each other, as

25 some measurements (Smith et al., 2002, Pope et al., 2005, Tatum Ernest et al., 2012) are

26 relative and normalized to absolute quantum yields (DeMore et al., 1997, Sander et al., 2011).

27 This influences the uncertainty range of the parameters A_i whose 1σ errors might be

28 somewhat larger than indicated in the respective equations.

29

30 page 5 / line 2

31 As Tatum Ernest et al. (2012) already indicated even the strong feature in Φ_{rad} at 321 nm

32 produces only a small change in the photolysis frequencies in the atmosphere. In fact

33 superposition of this feature on Equation 3 would increase j_{mol} by less than 2 % at all altitudes

1 and decrease j_{rad} by less than 4%, because it coincides with a small value in the absorption
2 coefficient of CH_2O .

3

4 page 9 / line 28

5 Its effect on the j_i is quite small – e.g. less than 0.3 % for j_{rad} – and included in the
6 calculations.

7

8 page 10 / line 11

9 The curve for $\sigma \cdot \Phi \cdot F_\lambda$ in Fig.4 nicely illustrates why the line structure observed by Tatum
10 Ernest et al. (2012) at 321 nm has so little impact on j_{mol} : It would increase the quite small
11 feature at 321 nm in that product by only a factor of 1.5.

12

13 page 10 / line 17

14 The calculations were made with 1 nm spectral resolution and are shown in Figure 5.

15

16 page 12 / added or changed references

17 Clark, J. H., Moore, C. B., and Nogar, N. S.: The photochemistry of formaldehyde: Absolute
18 quantum yields, radical reactions, and NO reactions, *J. Chem. Phys.*, 68, 1264 - 1271, 1978
19 DeMore, W. B., Sander, S. P., Howard, C. J., Ravishankara, A. R., Golden, D. M., Kolb, C.
20 E., Hampson, R. F., Kurylo, M. J., Molina, M. J.: NASA panel for data evaluation, chemical
21 kinetics and photochemical data evaluation for use in stratospheric modeling, JPL Publication
22 97-4, 1997

23 Gratien, A., Nilsson, E., Doussin, J.-F., Johnson, M. S., Nielsen, C. J., Stenstrom, Y., and
24 Picquet-Varrault, B.: UV and IR absorption cross-sections of HCHO, HCDO, and DCDO, *J.*
25 *Phys. Chem. A*, 111, 11506 - 11513, 2007

26 McQuigg, R. D. and Calvert, J. G.: The photodecomposition of CH_2O , CD_2O , CHDO , and
27 $\text{CH}_2\text{O}-\text{CD}_2\text{O}$ mixtures at Xenon flash lamp intensities, *J. Am. Chem. Soc.*, 91, 1590 – 1599,
28 1969

29 Tang, K. Y., Fairchild, P. W., and Lee, E. K. C.: Laser-induced photodecomposition of
30 formaldehyde (A^1A_2) from its single vibronic levels. Determination of the quantum yield of H
31 atom by HNO^* (A^1A'') chemiluminescence, *J. Phys. Chem.*, 83, 569 – 573, 1979

32

33

34 changes in tables and figures

1
2
3
4

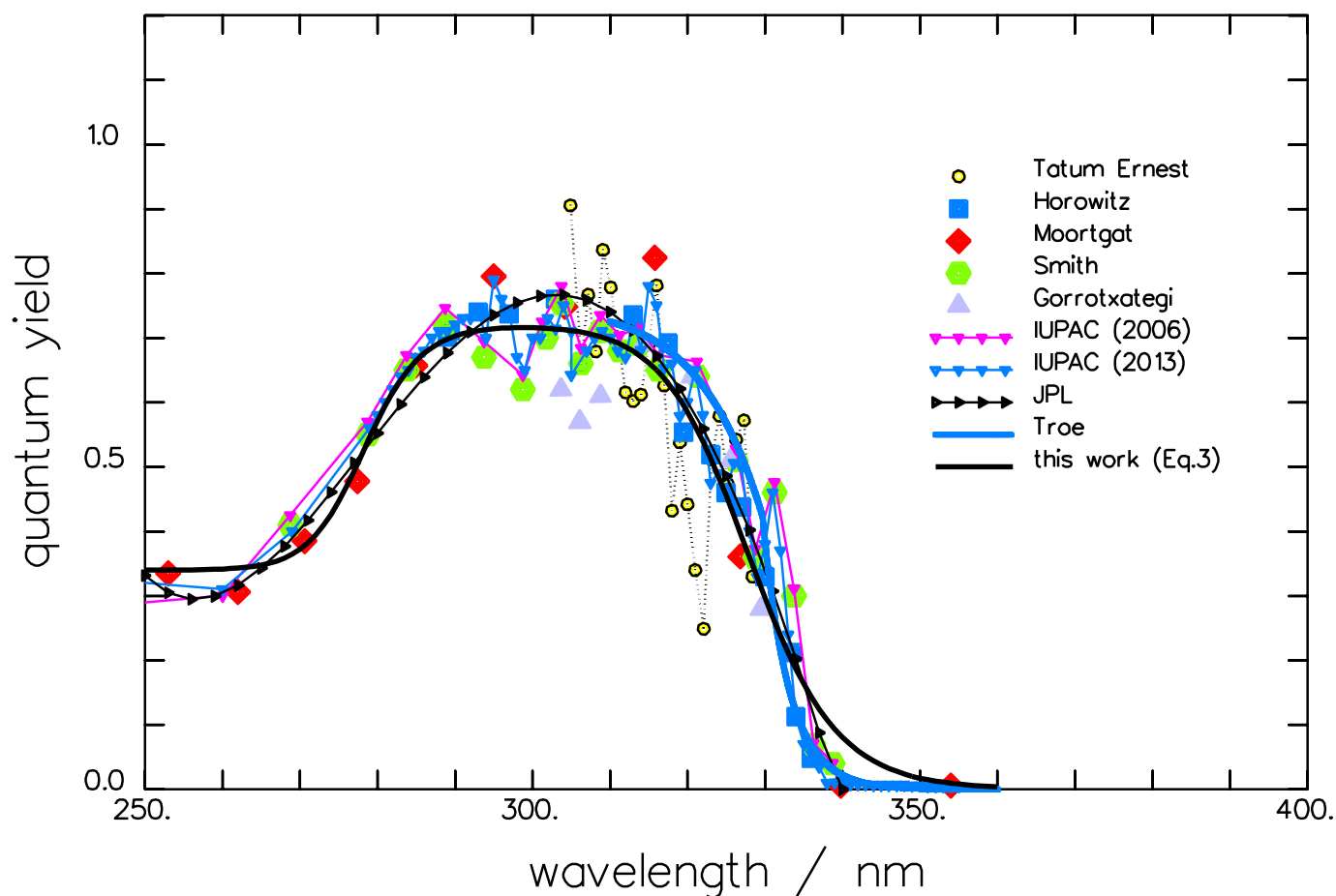
Table 1: Recommended quantum yield functions for use in atmospheric chemistry models (wavelength λ in nm).

$$\Phi_{rad} = \frac{0.74 \pm 0.01}{1 + \exp\left(\frac{-\left(\frac{1}{\lambda} - \frac{1}{327.4 \pm 0.5}\right)}{(5.4 \pm 0.5) \cdot 10^{-5}}\right)} - \frac{0.40 \pm 0.04}{1 + \exp\left(\frac{-\left(\frac{1}{\lambda} - \frac{1}{279.0 \pm 1.3}\right)}{(5.2 \pm 2.4) \cdot 10^{-5}}\right)} \quad (8)$$

$$\Phi_{tot} = \frac{1}{1 + \exp\left(\frac{-\left(\frac{1}{\lambda} - \frac{1}{346.9 \pm 0.5}\right)}{(5.4 \pm 0.3) \times 10^{-5}}\right)} \left(\frac{M}{M_0}\right) - \frac{0.22 \pm 0.02}{1 + \exp\left(\frac{-\left(\frac{1}{\lambda} - \frac{1}{279.0 \pm 1.3}\right)}{(5.2 \pm 2.4) \times 10^{-5}}\right)} \quad (9)$$

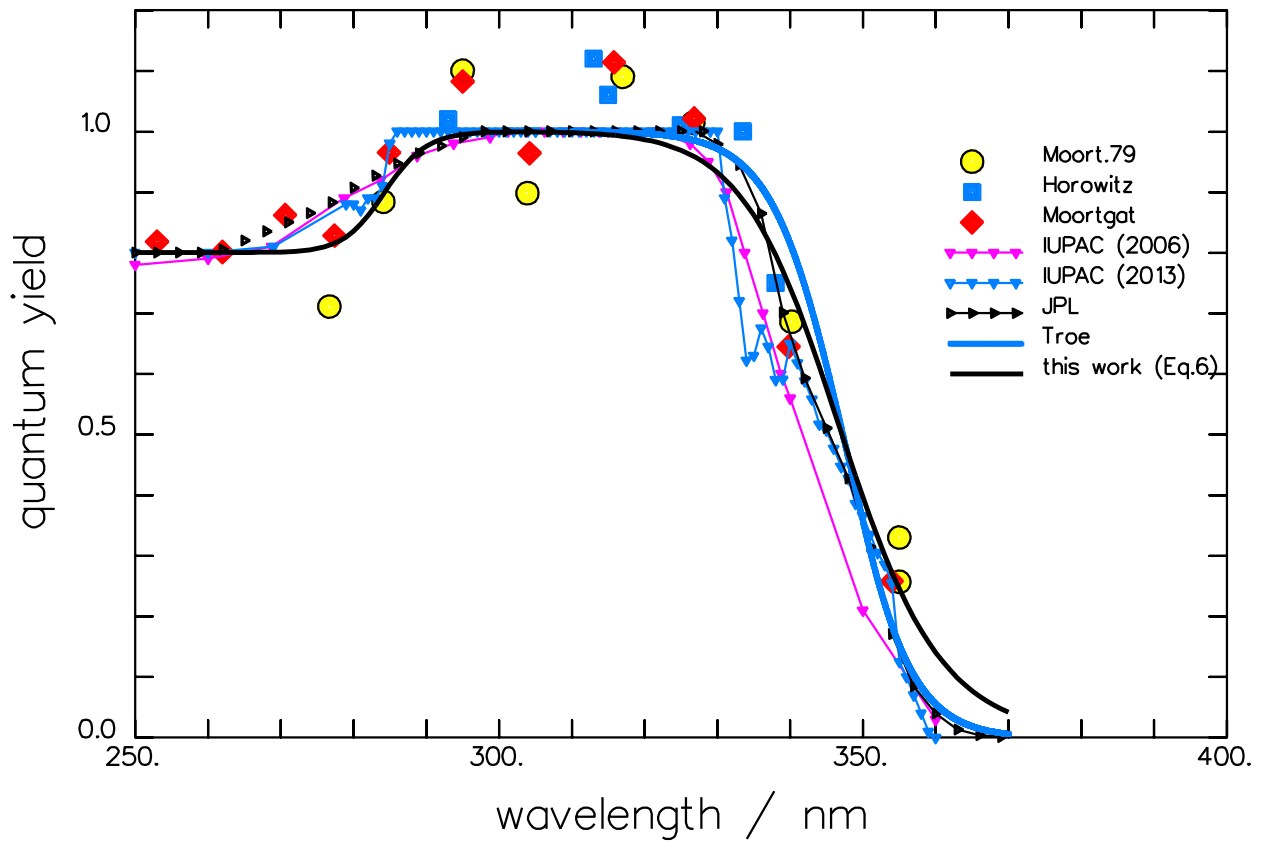
$$\Phi_{mol} = \frac{1}{1 + \exp\left(\frac{-\left(\frac{1}{\lambda} - \frac{1}{346.9 \pm 0.5}\right)}{(5.4 \pm 0.3) \times 10^{-5}}\right)} \left(\frac{M}{M_0}\right) - \frac{0.74 \pm 0.01}{1 + \exp\left(\frac{-\left(\frac{1}{\lambda} - \frac{1}{327.4 \pm 0.5}\right)}{(5.4 \pm 0.5) \cdot 10^{-5}}\right)} + \frac{0.18 \pm 0.02}{1 + \exp\left(\frac{-\left(\frac{1}{\lambda} - \frac{1}{279.0 \pm 1.3}\right)}{(5.2 \pm 2.4) \cdot 10^{-5}}\right)} \quad (10)$$

5
6
7



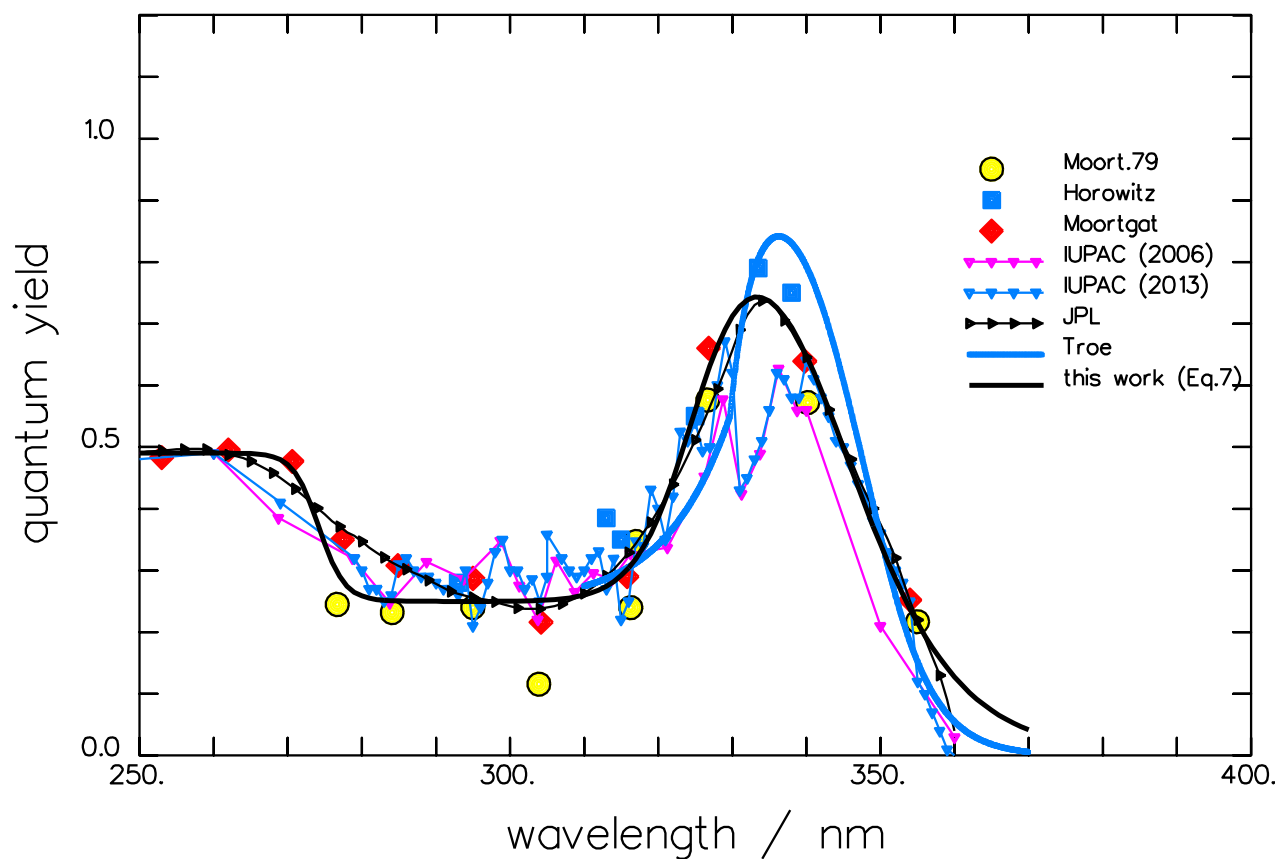
1
2
3
4 **Figure 1:** Spectrum of the quantum yield of the radical channel of the CH₂O photolysis at
5 room temperature. Measured data used for the fit are indicated by the large full symbols
6 (**Horowitz** and Calvert, 1978; **Moortgat** et al., 1983; **Smith** et al., 2002; **Gorrotxategi**
7 Carbajo et al., 2008). The present fit and the theoretical curve from **Troe** (2007) are given by
8 full lines. Recommended data are represented by small symbols connected by a thin line: **JPL**
9 (Sander et al., 2011); **IUPAC (2006)**, and **IUPAC (2013)**. The line structure observed by
10 **Tatum Ernest** et al. (2012) is indicated by open circles and a dotted line.

11



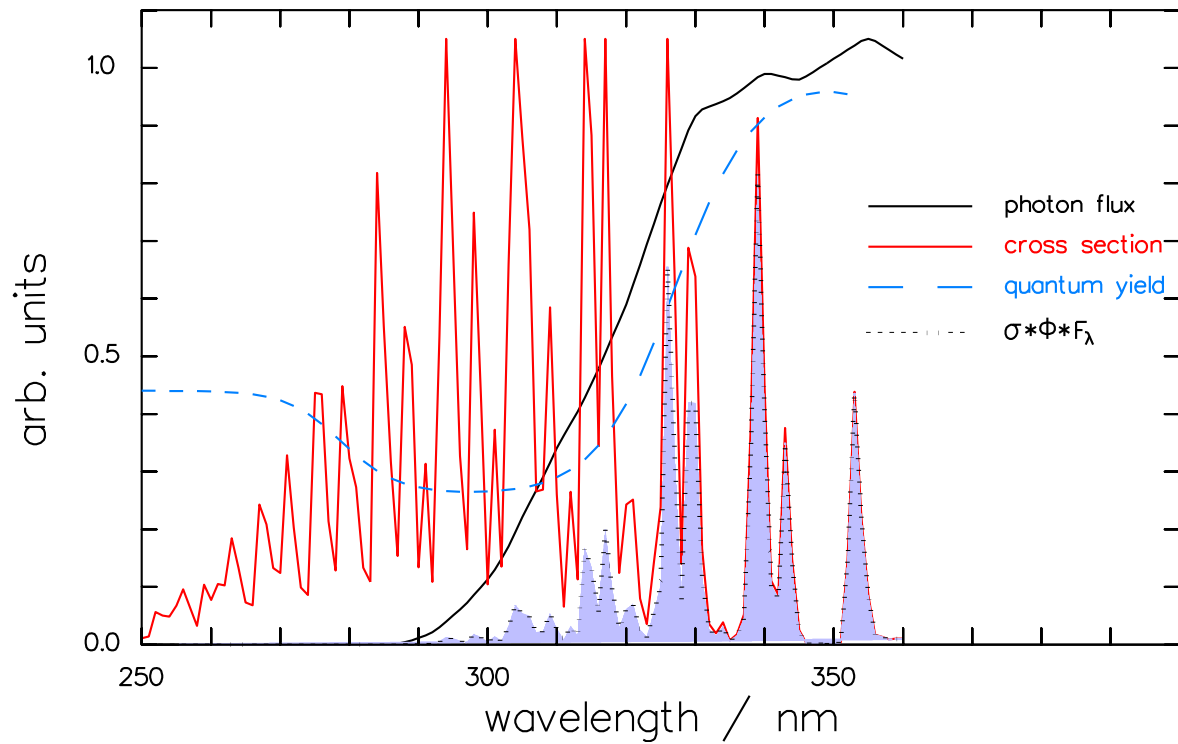
1
2
3
4
5
6
7
8
9
10
11

Figure 2: Spectrum of the quantum yield of the total CH₂O photolysis at room temperature. Measured data used for the fit are indicated by the large full symbols (**Moort.79:** Moortgat and Warneck, 1979, **Horowitz** and Calvert, 1978; **Moortgat** et al., 1983). The present fit and the theoretical curve from **Troe** (2007) are given by full lines. Recommended data are represented by small symbols connected by a thin line: **JPL** (Sander et al., 2011); **IUPAC (2006)**, and **IPUAC (2013)**.



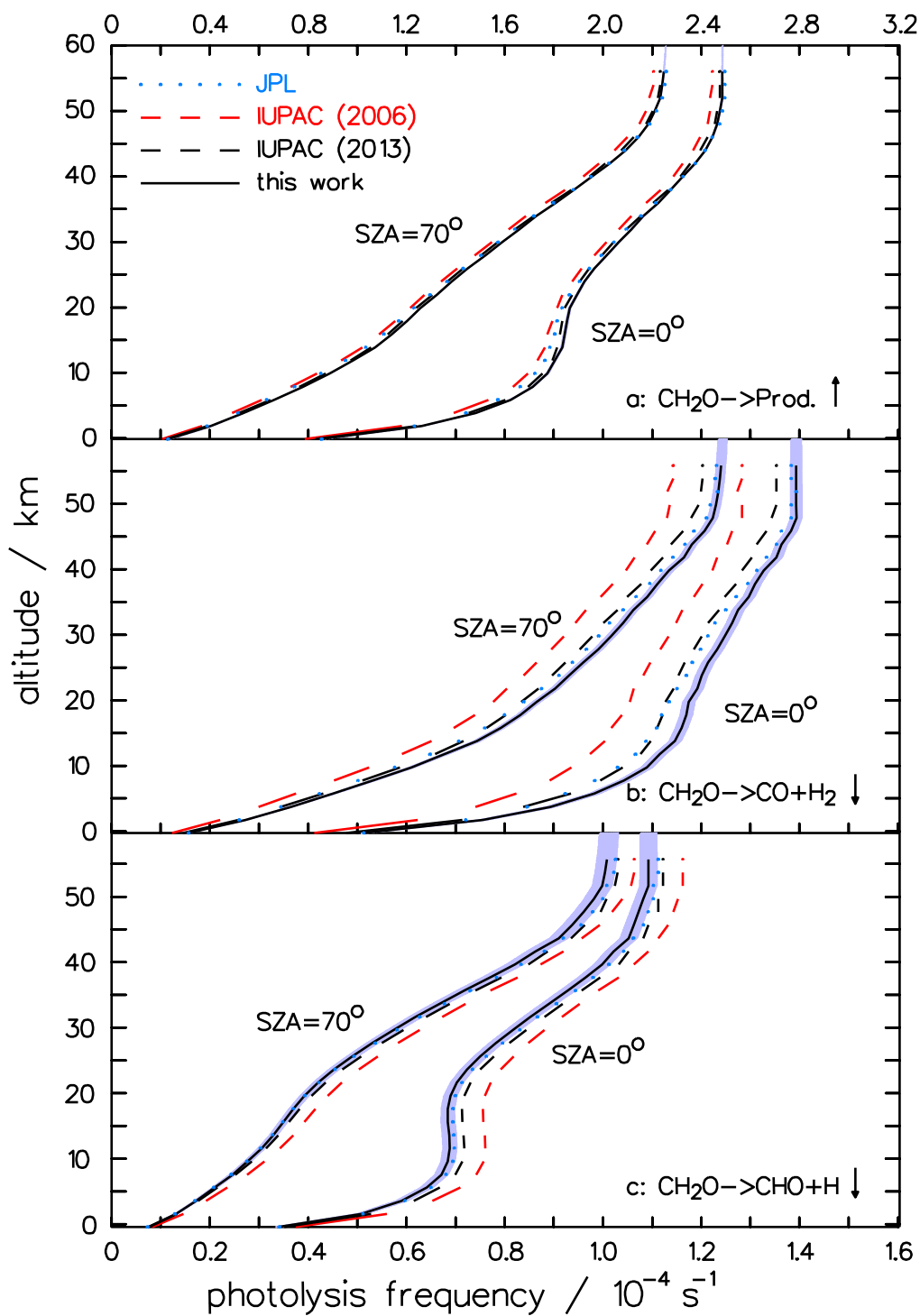
1
2
3
4
5
6
7
8
9
10
11

Figure 3: Spectrum of the quantum yield of the molecular branch of the CH₂O photolysis at room temperature. Measured data used for the fit are indicated by the large full symbols (**Moort.79:** Moortgat and Warneck, 1979, **Horowitz** and Calvert, 1978; **Moortgat** et al., 1983). The present fit and the theoretical curve from **Troe** (2007) are given by full lines. Recommended data are represented by small symbols connected by a thin line: **JPL** (Sander et al., 2011); **IUPAC (2006)**, and **IUPAC (2013)**.



1
2
3
4
5
6
7
8
9

Figure 4: Spectra of the actinic photon flux density (WMO, 1985), the optical absorption cross section (Gratien et al., 2007) and Φ_{mol} at 30 km altitude, 33° solar zenith angle, 227 K. The shaded area represents the integrand $\sigma \cdot \Phi \cdot F_\lambda$ of Eq.(11).



1
2

3 **Figure 6:** Comparison of the altitudinal profiles of the photolysis frequencies of
 4 formaldehyde from **JPL** (Sander et al., 2011); **IUPAC (2006)**, **IUPAC (2013)**, and the
 5 present work: total photolysis (a), molecular channel (b), and radical channel (c). The
 6 frequencies are depicted for two solar zenith angles (SZA). The shaded areas mark the 1σ
 7 error bounds of the profiles based on the errors of the fitting parameters for the present
 8 quantum yields. (The arrows point to the related ordinate)

1 A simple formulation of the CH₂O photolysis quantum yields

2

3 E.-P. Röth¹ and D. H. Ehhalt²

4 [1]{Institute for Energy and Climate Research (IEK-7: Stratosphere), Research Center Jülich,
5 Germany}

6 [2]{Institute for Energy and Climate Research (IEK-8: Troposphere), Research Center Jülich,
7 Germany}

8 Correspondence to: E.-P. Röth (e.p.roeth@fz-juelich.de)

9

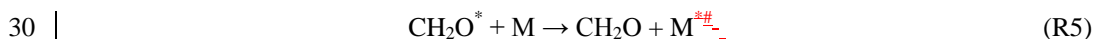
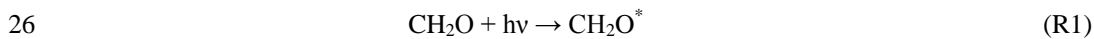
10 Abstract

11 New expressions for the ~~various-wavelength-wavelength~~-dependent photolysis quantum yields
12 of CH₂O, Φ_j , are presented. They are based on combinations of functions of the type
13 $A_i/(1+\exp[-(1/\lambda-1/\lambda_{0i})/b_i])^{-1}$. The parameters A_i , b_i , and λ_{0i} which have a physical meaning are
14 obtained by fits to the measured data of the Φ_j available from the literature. The altitude
15 dependence of the photolysis frequencies resulting from the new quantum yield expressions
16 are compared to those derived from the Φ_j recommended by JPL and IUPAC.

17

18 1. Introduction

19 Formaldehyde, CH₂O, is an important trace gas in the atmosphere. It is formed as an
20 intermediate in the oxidation of methane and non-methane hydrocarbons, and destroyed by
21 the reaction with OH and by photolysis in the near ultraviolet. The photolysis involves several
22 channels. Following the excitation (R1), CH₂O* can decay into purely molecular products
23 (R2), or into products that in the atmosphere lead to the eventual formation of hydroperoxy
24 radicals, HO₂, (R3, R4). The quenching reaction R5 and fluorescence R6 can influence the
25 quantum yields of the product channels.



32 As it turns out the molecular channel, R2, provides the by far largest source of molecular
33 hydrogen, H₂, in the atmosphere (Ehhalt and Rohrer, 2009). The radical channels, R3 and R4,
34 that generate HO₂ radicals, enhance local photochemistry. Finally each destruction of a CH₂O

1 molecule – including that by OH – eventually results in a carbon monoxide molecule, CO. As
2 a consequence, CH₂O is also an important source of CO in the atmosphere.

3 Recognizing the importance for atmospheric chemistry the quantum yields of the CH₂O
4 photolysis were measured early on and by various authors (see Sander et al., 2011, Atkinson
5 et al., 2006, and the internet version IUPAC (2013) for summaries).

6 The quantum yield Φ_{mol} of the molecular branch R2 was usually measured by monitoring the
7 H₂ production while scavenging the H atoms to prevent their contribution to the H₂
8 production (e.g., Moortgat et al., 1978, Horowitz and Calvert, 1978). The formation of the
9 molecular products via the reaction path of a roaming H-atom [see e.g., Bowman and Shepler,
10 2011 and Christoffel and Bowman, 2009] was not known then and is not included explicitly
11 in our list of reactions but it is included in reaction R2, and its quantum yield is part of the
12 measured Φ_{mol} .

13 Reactions R3 and R4 form the radical channel with the combined quantum yield Φ_{rad} which
14 in some cases was investigated directly by measuring the products, H and CHO (e.g., Smith
15 et al., 2002, Gorrotxategi et al., 2008, Tatum Ernest et al., 2012).

16 The fluorescence quantum yield (R6) was measured by Miller and Lee, 1978, in the
17 wavelength range 290 to 360 nm. Its maximum at 353 nm is less than 3.5 % and it is less than
18 1% at the other wavelengths considered. It will therefore be neglected here. We know of no
19 measurements below 290 nm.

20 The total quantum yield Φ_{tot} , i.e. the fraction of the decay of excited formaldehyde, CH₂O*,
21 into products other than its ground state, was derived from the CO production. By definition
22 Φ_{tot} is the sum of the quantum yields of the molecular and the radical channel:

$$\Phi_{\text{tot}} = \Phi_{\text{mol}} + \Phi_{\text{rad}} \quad (1)$$

24 The measured wavelength dependences of the quantum yields are usually given in tabular
25 form (see e.g., Atkinson et al., 2006, IUPAC, 2013). For Φ_{rad} also or as a fit by a fourth order
26 polynomial (see Sander et al., 2011) exists. To provide a more handy tool for atmospheric
27 modeling we propose to use combinations-sums of energy dependent functions of the type

$$\frac{A}{1 + \exp\left[\frac{-(1/\lambda - 1/\lambda_0)}{b}\right]} \quad (2)$$

29 to fit Φ_{mol} and Φ_{rad} . These functions are well-suited to map smooth transitions. They
30 allow to include pressure and temperature dependences. And the resulting parameters are few
31 and have a physical meaning; in particular $1/\lambda_0$ corresponds to the threshold energy of the
32 respective reaction; b describes the width of the transitions. Moreover, the formalism should
33 also provide a useful template for the formulation of the analogous Φ_i for the isotopologues of

1 formaldehyde. In particular we hope to eventually construct expressions of the quantum yields
2 for CHDO for which – apart from the threshold energies and a few isotope fractionation
3 factors- no direct measurements exist.

4 Our analysis of the quantum yields will be based on the data filed by JPL (Sander et al., 2011)
5 and IUPAC (2006) omitting all measurements ~~with an obvious bias whose wavelength~~
6 dependencies deviate strongly from the forms recommended by JPL or IUPAC (e.g.,
7 McQuigg and Calvert, Clark et al., Tang et al. for Φ_{rad}). Likewise, ~~only publications of~~
8 ~~independent measurements were taken into account, i.e.~~ if measured data appear in several
9 publications by the same authors, only the latest data were considered. Not all data are
10 independent of each other, as some measurements (Smith et al., 2002, Pope et al., 2005, Tatum
11 Ernest et al., 2012) are relative and normalized to absolute quantum yields (DeMore et al.,
12 1997, Sander et al., 2011). This influences the uncertainty range of the parameters A_i whose
13 1σ errors might be somewhat larger than indicated in the respective equations.

Formatiert: Nicht Hervorheben

14 First, in Sections 2 to 4, we will fit the measured wavelength dependences of the various Φ
15 separately and compare them to those reported in the literature. In a second step, after having
16 convinced ourselves that the parameters from the separate fits that should correspond to each
17 other are indeed similar in value, we attempt a simultaneous fit of all Φ in ~~chapter~~Chapter 5.

19 2. The quantum yield of the radical channel

20 Most publications on the formaldehyde photolysis deal with the radical channel R3 - notably:
21 Horowitz and Calvert (1978), Moortgat et al. (1983), Smith et al. (2002), Gorrotxategi et al.
22 (2008), and Tatum Ernest et al. (2012). Nearly all of these measurements were made at room
23 temperature, and experiments and theory indicate that there is no pressure dependence of Φ_{rad} .
24 We, therefore, assume all these data to be comparable and their variance attributable to
25 experimental error. Thus all these data are combined in Figure 1 ~~without any weighing~~. Smith
26 et al. (2002) attributed some of the variance in their data to a line structure in Φ_{rad} . The
27 possibility of a line structure ~~appears-is~~ corroborated by the data of Tatum Ernest et al. (2012),
28 which show a strong feature in Φ_{rad} at 321 nm. For comparison, the data of Tatum Ernest et al.
29 are also shown in Figure 1, but they are not used for the fit.

30 To fit the experimentally observed wavelength dependence of Φ_{rad} we use a combination of
31 two functions of the type mentioned above, one for the ~~long-wave~~ decay of Φ_{rad} to longer
32 wavelengths at about 328 nm, the other for the ~~short-wave~~ decay towards shorter wavelengths
33 at 277 nm. To obtain the fit parameters and their errors a simplex algorithm (Nelder and

1 Mead, 1965) is used in combination with a bootstrapping method with 2000 arbitrary
 2 removals of 20 % of the data. The result is given by Eq. (3), with λ in nm:

$$3 \quad \Phi_{rad} = \frac{0.72 \pm 0.01}{1 + \exp\left(\frac{-(1/\lambda - 1/328.0 \pm 0.6)}{(5.2 \pm 0.6) \cdot 10^{-5}}\right)} - \frac{0.38 \pm 0.03}{1 + \exp\left(\frac{-(1/\lambda - 1/278.4 \pm 0.8)}{(4.7 \pm 1.1) \cdot 10^{-5}}\right)} \quad (3)$$

4 ~~Eq. (3)~~ is also shown in Fig.1.

5 Eq. (3) holds primarily for room temperature. ~~Its first term defines the decay of Φ_{rad} to longer~~
 6 ~~wavelengths, its second term the decay towards shorter wavelengths.~~ The respective
 7 parameters will be labelled by the subscripts l,s. They stand for the short and long wavelength
 8 region. The index m, introduced below in Section 5 stands for the intermediate wavelength.

9 The λ_0 mark the inflection points in the decays: $\lambda_{0,l} = 328.0$ nm; $\lambda_{0,s} = 278.4$ nm. The
 10 corresponding b define the wavelength interval within which the decrease takes place. Owing
 11 to the scatter in the measured Φ_{rad} data all these parameters exhibit an uncertainty range. The
 12 estimated 1 σ errors are listed in Table 1 along with the values of the parameters of the
 13 parameters are also entered in Equation 3. We note that $\lambda_{0,l}$ closely corresponds to the
 14 dissociation energy of the H-CHO bond namely 30328.5 cm^{-1} or 329.7 nm (Terentis et al.,
 15 1998) and that $\lambda_{0,s}$ approximately corresponds to the heat of formation reaction of ~~reaction R4~~
 16 namely 423 kJ/mol or 283 nm (Sander et al., 2011).

17 Moortgat et al. (1983) have also measured the wavelength dependence of Φ_{rad} at 220 K. Given
 18 the experimental variance in those admittedly sparse data, Eq. (3) also fits the measured Φ_{rad}
 19 at 220 K quite well (not shown here). Thus, as far as the experimental data on Φ_{rad} are
 20 concerned, Eq. (3) covers the temperature range of 220 K to 300 K relevant for atmospheric
 21 modeling and there is no immediate need to introduce a temperature dependence. On the other
 22 hand, theoretical considerations suggest the inclusion of the internal energy of the CH₂O
 23 molecule, and this can be easily done: Following Troe (2007) one can add a term 3kT
 24 (appropriately scaled) to $1/\lambda$ in the left hand term of Eq. (3). In Section ~~6.5, Discussion,~~ we
 25 will investigate the impact of this T dependence (see Eq. 12) on the altitude profile of the
 26 respective photolysis frequency. In principle, another weak T dependence can arise through
 27 the parameter b. That dependence could be easily accommodated by replacing b by $(b_0 + b_1 T)$
 28 should future Φ_{rad} measurements provide enough information to warrant such a step.

29 The present formulation of Eq. (3) with constant parameters b - i.e. b independent of λ -
 30 forces the decrease to be nearly symmetrical around the respective λ_0 . This is not necessarily
 31 realistic. Again, if future measurements or theoretical considerations should prove the need,
 32 an asymmetry could be easily accommodated by allowing b to depend on λ .

1 Finally, we note, that a line structure could be superimposed on Eq. (3) without difficulty. For
2 the moment we refrain from doing so for two reasons: 1) As Tatum Ernest et al. (2012)
3 ~~showed already indicated~~ even the strong feature in Φ_{rad} at 321 nm ~~would produce only a~~
4 ~~small change in~~ the photolysis frequency ~~in the atmosphere~~, ~~j_{rad}~~ . ~~In fact, superposition of~~
5 ~~this feature on Equation 3 would increase j_{mol} by less than 2 % at all altitudes and decrease j_{rad}~~
6 ~~by less than, by only~~ 4%, because it coincides with a ~~strong small value~~ minimum in the
7 absorption coefficient of CH_2O . Thus the error possibly introduced by ~~its the~~ neglect of the
8 ~~line structure~~ is comparatively small (see discussion below). 2) The measurements of Φ_{rad} by
9 Smith et al. (2002), and Gorrotxategi et al. (2008) contain data points close to 321 nm which
10 fall right on the average Φ_{rad} given by Eq. (3). They were made with sufficient resolution to
11 resolve the feature at 321 nm and are therefore somewhat at variance with the finding of
12 Tatum Ernest et al. (2012).

13 Fig. 1 also contains the recommended wavelength dependences of Φ_{rad} given in the
14 evaluations by JPL (Sander et al., 2011), ~~and IUPAC (2006), and IUPAC (2013)~~. The reason
15 for the ~~choice inclusion~~ of IUPAC (2006) ~~over IUPAC (2013)~~ is that ~~the former~~ ~~these~~ data,
16 which were first published in 2002 and remained in the internet until 2012, had many users in
17 the past and possibly still ~~has have users~~ at present. Further included is the theory-based
18 dependence derived by Troe (2007); it covers only the restricted wavelength range from 310
19 to 350 nm. As a quantitative measure of the quality of these fits we ~~here add here~~ the
20 coefficient of determination ~~cd~~. In the present case this is identical to the correlation
21 coefficient between fitted and measured data. These correlation coefficients are: ~~cd~~ = 0.821
22 (IUPAC, 2006); ~~cd~~ = 0.840 (Troe, 2007); ~~cd~~ = 0.898 (JPL, 2011); ~~cd = 0.876 (IUPAC, 2013)~~,
23 and ~~cd~~ = 0.905 (this work); that is the quality of these various fits does not differ drastically.
24

25 3. The total quantum yield

26 There are more direct measurements for Φ_{tot} and its dependence on λ than for Φ_{mol} . To obtain
27 higher accuracy we, therefore, first obtain a fit for $\Phi_{\text{tot}}(\lambda)$ and then use Eq. (1), i.e. $\Phi_{\text{mol}} = \Phi_{\text{tot}}$
28 $- \Phi_{\text{rad}}$ for a fit of $\Phi_{\text{mol}}(\lambda)$. That fit is later compared to the measured dependence of Φ_{mol} on λ .
29 The available measurements of $\Phi_{\text{tot}}(\lambda)$ at 300 K temperature and 1013 hPa pressure are
30 reproduced in Figure 2. The values of Φ_{tot} at 355 nm and 353 nm were obtained by
31 interpolating the respective Stern-Volmer plots given by Moortgat et al. (1979, 1983) to the
32 pressure of 1 atm. The Φ_{tot} values at $\lambda < 340$ nm are pressure independent. The measured
33 $\Phi_{\text{tot}}(\lambda)$ exhibits three regions: a plateau between 290 and 330 nm, a steep decrease to zero at
34 longer wavelengths, and a weak decrease to $\Phi_{\text{tot}} \sim 0.8$ at shorter wavelengths. The average

1 measured Φ_{tot} in the plateau is 1.06 ± 0.09 – not significantly different from 1 – the maximum
 2 possible value. Therefore, in the fit we ~~will~~ fixed this value to unity. The separation of the two
 3 decreases by a plateau with $\Phi_{tot}=1$ also means that it is possible to fit these two regions of
 4 decrease separately and independently of each other.

5 The measurements in Figure 1 indicate that Φ_{rad} vanishes at $\lambda > 340$ nm; at those
 6 wavelengths Φ_{tot} becomes identical to Φ_{mol} . Moreover, tunneling processes extend the
 7 photolysis of CH_2O to H_2 and CO well beyond the threshold energy of about 350 nm (Troé,
 8 2007). In this energy regime the rate of decay into the molecular channel decreases to values
 9 where collisional quenching of the excited formaldehyde molecule (R5) begins to compete.
 10 Consequently, Φ_{mol} and Φ_{tot} become pressure dependent. Based on theoretical modeling and
 11 comparison with the data of Moortgat et al. (1978, 1983), Troé (2007) proposed a Stern-
 12 Volmer formulation for Φ_{mol} for $\lambda > 340$ nm:

$$13 \quad \Phi_{mol} = \frac{1}{1 + 1.4 \exp(c(\lambda - \lambda_0))(M/M_0)} \quad (4)$$

14 with $\lambda_0 = 349$ nm; $c = 0.225 \text{ nm}^{-1}$ for $\lambda > \lambda_0$ and $c = 0.205 \text{ nm}^{-1}$ for $\lambda < \lambda_0$ and M the number
 15 density of the bath gas. $M_0 = 2.46 \times 10^{19} \text{ cm}^{-3}$, the number density at 1013 hPa pressure and
 16 300 K temperature. Troé (2007) also pointed out that on theoretical grounds the temperature
 17 dependence of Φ_{mol} should be small compared to the experimental uncertainties and thus
 18 negligible at this stage. This is somewhat at variance to the measurements by Moortgat et al.
 19 (1983) which seem to indicate such a dependency, albeit with large uncertainties.

20 Since Φ_{tot} equals Φ_{mol} for $\lambda > 340$ nm where nearly all of the change in Φ_{tot} with wavelength
 21 is located, and since Eq. (4) approaches unity for $\lambda < 330$ nm, Eq. (4) should also provide a
 22 good approximation for $\Phi_{tot}(\lambda)$. In fact we could use it with its current parameters as our
 23 intended fit (see Figure 2).

24 However, we prefer to formulate our fit in terms of energy, i.e. $1/\lambda$. Moreover, a direct fit to
 25 the data in Figure 2 will merge the pre-exponential factor in Eq. (4) with λ_0 . So, instead of
 26 using Eq. (4) we will fit Eq. (5) to the data at $\lambda > 310$ nm in Figure 2:

$$27 \quad \Phi_{tot} = \frac{1}{1 + \exp\left(\frac{-\left(\frac{1}{\lambda} - \frac{1}{\lambda_{0,l}}\right)}{b_l}\right) \cdot (M/M_0)} \quad (5)$$

28 Our fit yields the parameters $\lambda_{0,l}$ and b_l of ~~Table 2~~ Eq.(6). In this case $\lambda_{0,l}$ has a somewhat
 29 different meaning than before. Here, $\lambda_{0,l}$ not only depends on the threshold energy of the
 30 reaction involved, but also on the quenching efficiency with which energy is drained from the

excited CH₂O molecule. But as before, $\lambda_{0,1}$ represents the inflection point in the decrease of Φ , at least for $M = M_0$.

The fit of Φ_{tot} for the short wave decrease relies on our model Eq. (2) and yields the parameters listed in Table 2 adds the second term in Eq. (6) for Φ_{tot} .

The equation for $\Phi_{tot}(\lambda)$ over the full wavelength range therefore is:

$$\Phi_{tot} = \frac{1}{1 + \exp\left(\frac{-(1/\lambda^{-1}/347.1 \pm 0.7)}{(5.7 \pm 0.8) \times 10^{-5}}\right)} \left(\frac{M}{M_0}\right) - \frac{0.20 \pm 0.01}{1 + \exp\left(\frac{-(1/\lambda^{-1}/284.3 \pm 0.9)}{(3.5 \pm 1.4) \times 10^{-5}}\right)} \quad (6)$$

with λ given in nm.

We have not been able to find a ready explanation for the experimentally observed weak decrease of Φ_{tot} at shorter wavelengths in the literature. We note, however, that $\lambda_{0,s}=284.3$ corresponds closely to the heat of formation reaction for R4 reaction (4) (see Section 2).

Following the arguments by Troe (2007) we assume the temperature dependence of $\Phi_{tot}(\lambda)$ to be negligible. But here again, our fitting functions could readily be modified to include a T dependence.

$\Phi_{tot}(\lambda)$ from Eq. (6) is also shown in Figure 2. It compares favorably to the measured data of Φ_{tot} . For additional comparison Figure 2 also contains the recommended wavelength dependences of Φ_{tot} given in the evaluations by JPL (Sander et al., 2011), IUPAC (2013), and IUPAC (2006). Further included is the dependence derived from Troe's (2007) Φ_{mol} ; it covers only the restricted wavelength range from 310 to 370 nm. Just as Eq. (6), the $\Phi_{tot}(\lambda)$ from JPL and that based on Troe (2007) agree well with the measurements. An exception are the recommended values from IUPAC (2006) which clearly deviate from the measurements in the range $330 \text{ nm} < \lambda < 350 \text{ nm}$. As a consequence of this deviation on the coefficient of determination is ~~poor~~ relatively small: $cd = 0.898913$, whereas the others are: JPL, $cd = 0.959$; Troe, $cd = 0.944$; present, $cd = 0.956$. In IUPAC (2013) this deviation is removed; the corresponding cd is 0.924.

4. The quantum yield of the molecular channel

Since Φ_{mol} is given by $\Phi_{tot} - \Phi_{rad}$, it could be simply obtained from the difference of Eqs. (6) and (3). Explicitly:

$$\Phi_{mol} = \Phi_{tot} - \Phi_{rad} = \frac{1}{1 + \exp\left(\frac{-(1/\lambda - 1/327.1)}{5.7 \times 10^{-5}}\right)} \left(\frac{M}{M_0}\right) - \frac{0.20}{1 + \exp\left(\frac{-(1/\lambda - 1/284.3)}{3.5 \times 10^{-5}}\right)} + \frac{0.72}{1 + \exp\left(\frac{-(1/\lambda - 1/328.0)}{5.2 \times 10^{-5}}\right)} + \frac{0.38}{1 + \exp\left(\frac{-(1/\lambda - 1/278.4)}{4.7 \times 10^{-5}}\right)} \quad (7)$$

On the other hand, Φ_{mol} can be obtained by a direct fit to the measured data. This requires a combination of only three functions of the Eq. (2) type and the fit results in:

$$\Phi_{mol} = \frac{1}{1 + \exp\left(\frac{-(1/\lambda - 1/345.2 \pm 0.8)}{(6.2 \pm 1.7) \times 10^{-5}}\right)} \left(\frac{M}{M_0}\right) - \frac{0.75 \pm 0.03}{1 + \exp\left(\frac{-(1/\lambda - 1/325.3 \pm 0.6)}{(3.9 \pm 0.5) \times 10^{-5}}\right)} + \frac{0.24 \pm 0.05}{1 + \exp\left(\frac{-(1/\lambda - 1/274.2 \pm 3.3)}{(2.3 \pm 2.1) \cdot 10^{-5}}\right)} \quad (87)$$

Eq. (87) makes the implicit assumption that the short wave decreases in Φ_{tot} and Φ_{rad} (second and fourth term in Eq. (7)) have the same $\lambda_{0,s}$ and b_s . The estimated 1σ errors along with of the fit parameters are listed in Table 3 entered in Eq. (7).

In Figure 3, $\Phi_{mol}(\lambda)$ from Eq. (87) is compared to the measured data on $\Phi_{mol}(\lambda)$. The latter consist of direct measurements of Φ_{mol} by Moortgat et al. (1979; 1983), and data based on measured Φ_{tot} and Φ_{rad} by Horowitz and Calvert (1978). The agreement of Eq. (87) with the measurements is quite reasonable. For further comparison Figure 3 also includes the recommendations by JPL (Sander et al., 2011), IUPAC (2013), and IUPAC (2006) as well as a fit based on Φ_{tot} and Φ_{rad} derived from Troe (2007). The respective coefficients of determination are: $c_d = 0.822$ (IUPAC, 2006); $c_d = 0.838$ (Troe, 2007); $c_d = 0.947$ (JPL; 2011); $c_d = 0.843$ (IUPAC, 2013); $c_d = 0.958$ (this work); IUPAC (2013) would yield $c = 0.843$.

5. Simultaneous fit of Φ_{rad} , Φ_{mol} , and Φ_{tot}

A comparison of the parameters and their errors obtained from the individual fits of the various Φ suggests that the $\lambda_{0,s}$, $\lambda_{0,m}$, $\lambda_{0,l}$ and b_s , b_m , b_l in a given fit equation do not differ significantly from the corresponding parameters in the others. We felt, therefore, felt justified to attempt a simultaneous fit of all Φ . In this attempt we assume that the corresponding λ_0 and b parameters in the various equations for Φ are indeed identical. We further assume that Φ_{tot} reaches a maximum value of 1 and that Eq. (1) holds. With these assumptions the total number of fit parameters for all three Φ together reduces to 9. The simultaneous calculation of

1 the 9 unknown parameters results in the equations for the Φ_i listed in Table 4-1. The
2 ~~coefficients of determination their estimated 1 σ errors are also entered in the~~
3 ~~equation together with the function parameters and their estimated 1 σ errors are tabulated in~~
4 ~~Table 5.~~

5 The functions of Table 4-1 differ somewhat, but hardly significantly from those given by Eqs.
6 (3), (6) and (87) considering the experimental uncertainties. The coefficients of determination
7 are comparable to those from the individual fits: $c=0.904$ for Φ_{rad} , 0.951 for Φ_{tot} , and 0.934 for
8 Φ_{mol} . ~~The relative errors of the parameters of Φ_{tot} of the shortwave decay are identical to~~
9 ~~those of Φ_{rad} by definition, as it is the case for the errors of the Φ_{mol} function.~~ Because of
10 their simplicity Eqs. (9), (108), and (110) represent our preferred formulation of the CH₂O
11 quantum yields and will be used in the discussion below.

12

13 6. Discussion

14 In the foregoing sections we presented new formulations of Φ_{tot} , Φ_{rad} , and Φ_{mol} for CH₂O. The
15 presentation also made it ~~also~~ clear that there is room for improvements. One concerns the
16 temperature dependence of Φ . Given the experimental uncertainties we have refrained from
17 providing T dependences for the Φ 's. But there are temperature dependences in the literature,
18 which could be incorporated in our formulation (Atkinson et al., 2006; Troe, 2007; Sander et
19 al., 2011). Below we will incorporate such a temperature dependence in Φ_{rad} to test the
20 sensitivity of the corresponding photolysis frequencies of CH₂O to the vertical temperature
21 profile.

22 In addition, the question of line structure in Φ_{rad} needs eventually to be resolved.

23 Of major interest to the atmospheric chemists is the impact of this new formulation of Φ on
24 the atmospheric photolysis frequencies of CH₂O. That photolysis frequency j is given by:

$$25 \quad j = \int_0^{\infty} \Phi(\lambda) \sigma(\lambda) F_{\lambda}(\lambda) d\lambda \quad (121)$$

26 i.e. it also depends on the absorption cross-section, $\sigma(\lambda)$, of CH₂O, and the local actinic
27 photon flux density $F_{\lambda}(\lambda)$. For our calculations of j we will use the absorption spectrum
28 measured by Gratien et al. (2007). It is, by the way, also slightly temperature dependent; the
29 respective function can be found in Röth et al. (1997). Its effect on the j_i is quite small – e.g.
30 less than 0.3 % for j_{rad} – and included in the calculations. The atmospheric actinic photon flux
31 density consists of down-welling and up-welling contributions, and depends of course on the
32 solar zenith angle and altitude. It was calculated by the radiative transfer program ART (Röth,
33 2002) using the extraterrestrial solar flux from WMO (1985). All three factors under the

1 integral strongly vary with wavelength, λ . (To various degrees they also vary with altitude.)
2 As an example Figure 4 shows $\sigma(\lambda)$, $F_\lambda(\lambda)$, and $\Phi_{\text{mol}}(\lambda)$, together with the wavelength
3 dependent integrand of Eq.(11) at 30 km altitude and 33° solar zenith angle. We particularly
4 notice the sharp cutoff in $F_\lambda(\lambda)$ around $\lambda = 320$ nm caused by the absorption of solar UV in
5 the ozone layer at lower wavelengths. This means that below 30 km altitude the exact form of
6 the Φ_i at $\lambda < 300$ nm has little influence on the various photolysis frequencies. Figure 4
7 further indicates how much the long-wave decrease of Φ_{mol} is shifted towards longer
8 wavelengths at the air density at 30 km altitude. In fact, this shift is so large that the long-
9 wave cutoff of the integrand in Eq. (11) is no longer determined by Φ_{mol} , as it is at low
10 altitudes, but rather by the absorption spectrum of CH_2O . Hence, at altitudes above 30 km the
11 exact form of the decrease in Φ_{mol} and Φ_{tot} at the longer wavelengths has no influence on the
12 respective photolysis frequencies. The curve for $\sigma \cdot \Phi \cdot F_\lambda$ in Fig.4 nicely illustrates why the line
13 structure observed by Tatum Ernest et al. (2012) at 321 nm has so little impact on j_{mol} : It
14 would increase the quite small feature at 321 nm in that product by only a factor of 1.5.
15 Given the Φ_i from the Eqs. (89) to (110) in Table 1, $\sigma(\lambda)$ from Gratien et al. (2007) along
16 with vertical temperature and density profiles of the U.S. standard atmosphere (NOAA, 1976)
17 we can calculate the vertical profiles of the photolysis rates. They are shown in Figure 5
18 calculations were made with 1 nm spectral resolution and are shown in Figure 5. The shaded
19 areas mark the 1σ error bounds of the j_i profiles based on the errors of the fitting parameters
20 for Φ_i given in Section 5. As to be expected, all j_i increase with altitude. In the case of j_{rad} that
21 increase is essentially due to the vertical change in $F_\lambda(\lambda)$, since our Φ_{rad} is neither temperature
22 nor pressure dependent and thus independent of altitude, and the slight temperature
23 dependence of $\sigma(\lambda)$ makes a minor contribution only. j_{tot} and j_{mol} , however, are significantly
24 modified by the density dependence in Φ_{mol} .
25 In Figure 5 we also demonstrate the impact of a possible temperature dependence in Φ_{rad} . The
26 temperature dependence is introduced by adding the term $(300-T)(3k/hc)$ in the appropriate
27 dimensional units to $1/\lambda$ in the first term of Eq. (3) (see Troe, 2007, and Section 2.).

Formatiert: Tiefgestellt

$$\Phi_{\text{rad}} = \frac{0.74}{1 + \exp\left(\frac{-\left(\frac{1}{\lambda} + (300-T)\left(\frac{3k}{hc}\right) - \frac{1}{327.4}\right)}{5.4 \cdot 10^{-5}}\right)} - \frac{0.40}{1 + \exp\left(\frac{-\left(\frac{1}{\lambda} - \frac{1}{279.0}\right)}{5.2 \cdot 10^{-5}}\right)}$$

(1312)

29 ~~That means: Only~~ This means that only the long-wave decay in Φ_{rad} is considered to be
30 temperature dependent. Here k is the Boltzmann constant, h the Planck constant, and c the
31 speed of light. As Figure 5 shows, a temperature dependence of this size clearly has a
32

1 significant impact on j_{rad} and by virtue of $\Phi_{\text{mol}} = \Phi_{\text{tot}} - \Phi_{\text{rad}}$ also on j_{mol} . The effect is largest at
2 around 15 km, the height of the temperature minimum, and about -9% for j_{rad} , respectively ca.
3 +6% for j_{mol} . The temperature at 15 km is 220 K, i.e. the temperature shifts in j_{rad} and j_{mol}
4 correspond to a temperature difference of 80 K. Apparently a correct formulation of the T-
5 dependence of Φ_{rad} could lead to a significant ~~improvement~~ change in the predicted vertical
6 profiles of j_{rad} and j_{mol} .
7 j_{tot} remains unaffected by the proposed temperature dependency. In fact, even assuming a
8 temperature dependence of the kind above for the long-wave decay of Φ_{tot} would have
9 comparatively little impact on the j_{tot} profile. It would be masked by the air density
10 dependence of Φ_{tot} . Just as at lower densities, the exact form of the long-wave decay in Φ_{tot}
11 no longer influences j_{tot} , so can its temperature dependence no longer influence j_{tot} .
12 Finally, in Figure 6, we compare the photolysis frequencies based on this work's quantum
13 yields to those calculated with the quantum yields recommended by IUPAC (2006), IUPAC
14 (2013), and JPL (Sander et al., 2011). The JPL recommendation includes an explicit
15 temperature dependence for Φ_{rad} . In addition, both, JPL and IUPAC (2006), treat the density
16 dependence of Φ_{mol} in terms of atmospheric pressure, which introduces a further temperature
17 dependence. Both temperature effects are included in the calculation of the respective j_i
18 profiles. The comparison demonstrates that even at present – without a representation of the
19 temperature dependence - our Φ_i provide vertical profiles of the photolysis frequency which
20 agree well with those based on Φ_i from the JPL recommendation - for all j_i and both solar
21 zenith angles considered. The comparison with the data from Atkinson et al. (2006) is less
22 favorable, especially for j_{mol} . This reflects the differences between $\Phi_{\text{mol}}(\lambda)$ given here and
23 that recommended by JPL on the one hand to that recommended by Atkinson et al. (2006) on
24 the other, which were already apparent in Figures 2 and 3. The new quantum yields
25 recommended by IUPAC in 2013 give photolysis rates which lie slightly ~~above~~ below our
26 ~~values~~ curves for j_{mol} , just outside the error bounds.
27 Although the derived j_i profiles as well as the fits to the measured Φ_i (Figures 1 to 3) based on
28 the JPL recommendation and on the present work appear reasonably equivalent, we feel ~~our~~
29 formalism to be advantageous. Since it consistently formulates the wavelength dependence
30 of Φ_i in terms of $1/\lambda$, its fitting parameters are in units of energy, and represent, or are close
31 to, molecular parameters, notably threshold energies, which are often available and can serve
32 as guides. Moreover, the formulation in units of energy makes it easy to introduce
33 temperature dependences should future measurements or theoretical considerations demand it.
34 For the same reasons our formalism should provide a useful template for the formulation of

1 the Φ_i for the isotopologues of formaldehyde and likewise for the photolysis quantum yields
2 of many other molecules.

3 Acknowledgement

4 The article processing charges for this open-access publication have been covered by a
5 Research Centre of the Helmholtz Association.

6 **References**

- 7 Atkinson, R., Baulch, D. L., Cox, R. A., Crowley, J. N., Hampson, R. F., Hynes, R. G.,
8 Jenkin, M. E., Rossi, M. F., and Troe, J.: Evaluated kinetic and photochemical data for
9 atmospheric chemistry: Volume II – gas phase reactions of organic species, Atmos. Chem.
10 Phys., 6, 3625 – 4055, 2006
- 11 Bowman, J. M. and Shepler, B. C.: Roaming Radicals, Ann. Rev. Phys. Chem., 62, 531 –
12 553, 2011
- 13 Christoffel, K. M. and Bowman, J. M.: Three Reaction Pathways in the $H + HCO \rightarrow H_2 + CO$
14 Reaction, J. Phys. Chem. A, 113, 4138 – 4144, 2009
- 15 Clark, J. H., Moore, C. B., and Nogar, N. S.: The photochemistry of formaldehyde: Absolute
16 quantum yields, radical reactions, and NO reactions, J. Chem. Phys., 68, 1264 - 1271, 1978
17 DeMore, W. B., Sander, S. P., Howard, C. J., Ravishankara, A. R., Golden, D. M., Kolb, C.
18 E., Hampson, R. F., Kurylo, M. J., Molina, M. J.: NASA panel for data evaluation, chemical
19 kinetics and photochemical data evaluation for use in stratospheric modeling, JPL Publication
20 97-4, 1997
- 21 Gorrotxategi Carbajo, P., Smith, S. C., Holloway, A. L., Smith, C. A., Pope, F. D.,
22 Shallcross, D. E., and Orr-Ewing, A. J.: Ultraviolet photolysis of HCHO: Absolute HCO
23 quantum yields by direct detection of the HCO Radical photoproduct, J. Phys. Chem. A, 112,
24 12437 – 12448, 2008
- 25 Gratien, A., Picquet Varrault, B., Orphal, J., Perrandin, E., Doussin, J. F., and Flaud, J. M.:
26 Laboratory intercomparison of the formaldehyde absorption cross sections in the infrared
27 (1660–1820 cm^{-1}) and ultraviolet (300–360 nm) spectral region, J. Geophys. Res., 112,
28 D05305, doi:10.1029/2006JD007201
- 29 Nilsson, E., Doussin, J.-F., Johnson, M. S., Nielsen, C.
30 J., Stenstrom, Y., and Picquet-Varrault, B.: UV and IR absorption cross-sections of HCHO,
31 HCDO, and DCDO, J. Phys. Chem. A, 111, 11506 - 11513, 2007

Formatiert: Zeilenabstand: 1,5 Zeilen

Formatiert: Schriftart: Fett

1 | Horowitz, A. and Calvert, J. ~~CG~~: Wavelength dependence of the quantum efficiencies of the
2 | primary processes in formaldehyde photolysis at 25°C. Int. J. Chem. Kinetics, 10, 805 – 819,
3 | 1978
4 | IUPAC (2006) : see Atkinson et al. (2006)
5 | IUPAC (2013): IUPAC Task Group on Atmospheric Chemical Kinetic Data Evaluation –
6 | Data Sheet P1, <http://iupac.pole-ether.fr>, (last access: 16 January 2015) 2013
7 | [McQuigg, R. D. and Calvert, J. G.: The photodecomposition of CH₂O, CD₂O, CHDO, and](#)
8 | [CH₂O-CD₂O mixtures at Xenon flash lamp intensities, J. Am. Chem. Soc., 91, 1590 – 1599,](#)
9 | [1969](#)
10 | Miller, R. G. and Lee, E. K. C.: Single vibronic level photochemistry of formaldehyde~~s~~ in the
11 | A¹A₂ state: Radiative and non radiative processes in H₂CO, HDCO, and D₂O, J. Chem. Phys.,
12 | 68, 4448 – 4464, 1978
13 | Moortgat, G. K., Slemr, F., Seiler, W., and Warneck, P.: Photolysis of formaldehyde: Relative
14 | quantum yields of H₂ and CO in the wavelength range 270 -360 nm, Chem. Phys. Letters, 54,
15 | 444 – 447, 1978
16 | Moortgat, G. K. and Warneck, P.: CO and H₂ quantum yields in the photodecomposition of
17 | formaldehyde in air, J. Chem. Phys., 70, 3639 – 3651, 1979
18 | Moortgat, G. K., Seiler, W., and Warneck, P.: Photodissociation of HCHO in air: CO and H₂
19 | quantum yields at 220 K and 300 K, J. Chem. Phys., 78, 1185 – 1190, 1983
20 | Nelder, J. A. and Mead, R.: A simplex method for function minimization, Computer Journal,
21 | 7, 308 -313, 1965
22 | NOAA,; U.S. Standard Atmosphere, NOAA-S/T76-1562, [Washington D.C.](#), 1976
23 | Röth, E.-P.: Description of the anisotropic radiation transfer model ART to determine
24 | photodissociation coefficients, Ber. Forschungszentrum Jülich, Jül-3960, [Jülich](#), 2002
25 | Röth, E.-P., Ruhnke, R., Moortgat, G., Meller, R., and Schneider, W.: UV/VIS ~~Absorption~~
26 | ~~absorption~~ ~~Cross-cross~~ ~~Sections-sections~~ and ~~Quantum-quantum~~ ~~Yields-yields~~ for ~~Use-use~~ in
27 | ~~Photochemistry-photochemistry~~ and ~~Atmospheric-atmospheric~~ ~~Modelingmodeling~~. Part 2:
28 | Organic ~~Substanceessubstances~~, Ber. Forschungszentrum Jülich, Jül-3341, [Jülich](#), 1997
29 | Sander, S. P., Friedl, R.R., Abbatt, J. P. D., Barker, J. R., Burkholder, J. B., Golden, D. M.,
30 | Kolb, C. E., Kurylo, M. J., Moortgat, G. K., Wine, P. H., Huie, R. E., and Orkin, V. L.:
31 | Chemical kinetics and photochemical data for use in atmospheric studies. Evaluation number
32 | 17, JPL-Publication 10-6, [Pasadena](#), 2011

1 | Smith, G. D., Molina, L. T., and Molina, ~~N.M.~~ J.: Measurement of radical quantum yields ~~for~~
2 | from formaldehyde photolysis between 269 and 339 nm, J. Phys. Chem. A, 106, 1233 – 1240,
3 | 2002
4 | Tang, K. Y., Fairchild, P. W., and Lee, E. K. C.: Laser-induced photodecomposition of
5 | formaldehyde (A^1A_2) from its single vibronic levels. Determination of the quantum yield of H
6 | atom by HNO^* (A^1A'') chemiluminescence, J. Phys. Chem., 83, 569 – 573, 1979
7 | Tatum Ernest, C., Bauer, D., and Hynes, A. J.: Radical Quantum Yields from Formaldehyde
8 | Photolysis in the 30 300 – 32 890 cm^{-1} (304 – 329 nm) Spectral Region: Detection of Radical
9 | Products Using Pulsed Laser Photolysis – Pulsed Laser Induced Fluorescence, J. Phys. Chem.
10 | A, 116, 6983 – 6995, 2012
11 | Terentis, A. C., Waugh, S. E., Metha, G. F., and Kable, S. H.: HCO (N, K_a, K_c, J) distributions
12 | from near-threshold photolysis of H_2CO (J, K_a, K_c), J. Chem. Phys. 108, 3187 – 3198, 1998
13 | Troe, J.: Analysis of quantum yields for the photolysis of formaldehyde at $\lambda > 310$ nm, J.
14 | Phys. Chem. A, 111, 3868 – 3874, 2007
15 | WMO: Atmospheric Ozone 1985, Vol. 1, WNO Report 16, Genf, 1985
16

1
2 **Table 1:** Coefficients of the quantum yield function for the radical channel and 1- σ errors of
3 Eq. 3.
4

coefficient	value	error
A_1	0.72	± 0.01
$\lambda_{0,1}$	328.0 nm	± 0.6 nm
b_1	$5.2 \times 10^{-5} \text{ nm}^{-1}$	$\pm 0.6 \times 10^{-5} \text{ nm}^{-1}$
A_3	0.38	± 0.03
$\lambda_{0,3}$	278.4 nm	± 0.8 nm
b_3	$4.7 \times 10^{-5} \text{ nm}^{-1}$	$\pm 1.1 \times 10^{-5} \text{ nm}^{-1}$

5
6

1
2
3
4
5

Table 2: Coefficients of the total quantum yield function and $1-\sigma$ errors of Eq. 6.

coefficient	value	error
A_t	1.0	fixed
$\lambda_{0,t}$	347.1 nm	± 0.7 nm
b_t	$5.7 \times 10^{-5} \text{ nm}^{-1}$	$\pm 0.8 \times 10^{-5} \text{ nm}^{-1}$
A_s	0.20	± 0.01
$\lambda_{0,s}$	284.3 nm	± 0.9 nm
b_s	$3.5 \times 10^{-5} \text{ nm}^{-1}$	$\pm 1.4 \times 10^{-5} \text{ nm}^{-1}$

1
2 **Table 3:** Coefficients of the quantum yield function for the molecular channel and 1- σ errors
3 of Eq. 8.
4

coefficient	value	error
A_l	1.0	fixed
$\lambda_{0,l}$	345.2 nm	± 0.8 nm
b_l	$6.2 \times 10^{-5} \text{ nm}^{-1}$	$\pm 1.7 \times 10^{-5} \text{ nm}^{-1}$
A_m	0.75	± 0.03
$\lambda_{0,m}$	325.3 nm	± 0.6 nm
b_m	$3.9 \times 10^{-5} \text{ nm}^{-1}$	$\pm 0.5 \times 10^{-5} \text{ nm}^{-1}$
A_s	0.24	± 0.05
$\lambda_{0,s}$	274.2 nm	± 3.3 nm
b_s	$2.3 \times 10^{-5} \text{ nm}^{-1}$	$\pm 2.1 \times 10^{-5} \text{ nm}^{-1}$

5
6

1
2 | **Table 41:** Recommended quantum yield functions for use in atmospheric chemistry models
3 (wavelength λ in nm).
4

$$\Phi_{rad} = \frac{0.74 \pm 0.01}{1 + \exp\left(\frac{-(1/\lambda - 1/327.4 \pm 0.5)}{(5.4 \pm 0.5) \cdot 10^{-5}}\right)} - \frac{0.40 \pm 0.04}{1 + \exp\left(\frac{-(1/\lambda - 1/279.0 \pm 1.3)}{(5.2 \pm 2.4) \cdot 10^{-5}}\right)} \quad (98)$$

$$\Phi_{tot} = \frac{1}{1 + \exp\left(\frac{-(1/\lambda - 1/346.9 \pm 0.5)}{(5.4 \pm 0.3) \times 10^{-5}}\right)} (M/M_0) - \frac{0.22 \pm 0.02}{1 + \exp\left(\frac{-(1/\lambda - 1/279.0 \pm 1.3)}{(5.2 \pm 2.4) \times 10^{-5}}\right)} \quad (109)$$

$$\Phi_{mol} = \frac{1}{1 + \exp\left(\frac{-(1/\lambda - 1/346.9 \pm 0.5)}{(5.4 \pm 0.3) \times 10^{-5}}\right)} (M/M_0) - \frac{0.74 \pm 0.01}{1 + \exp\left(\frac{-(1/\lambda - 1/327.4 \pm 0.5)}{(5.4 \pm 0.5) \cdot 10^{-5}}\right)} + \frac{0.18 \pm 0.02}{1 + \exp\left(\frac{-(1/\lambda - 1/279.0 \pm 1.3)}{(5.2 \pm 2.4) \cdot 10^{-5}}\right)} \quad (110)$$

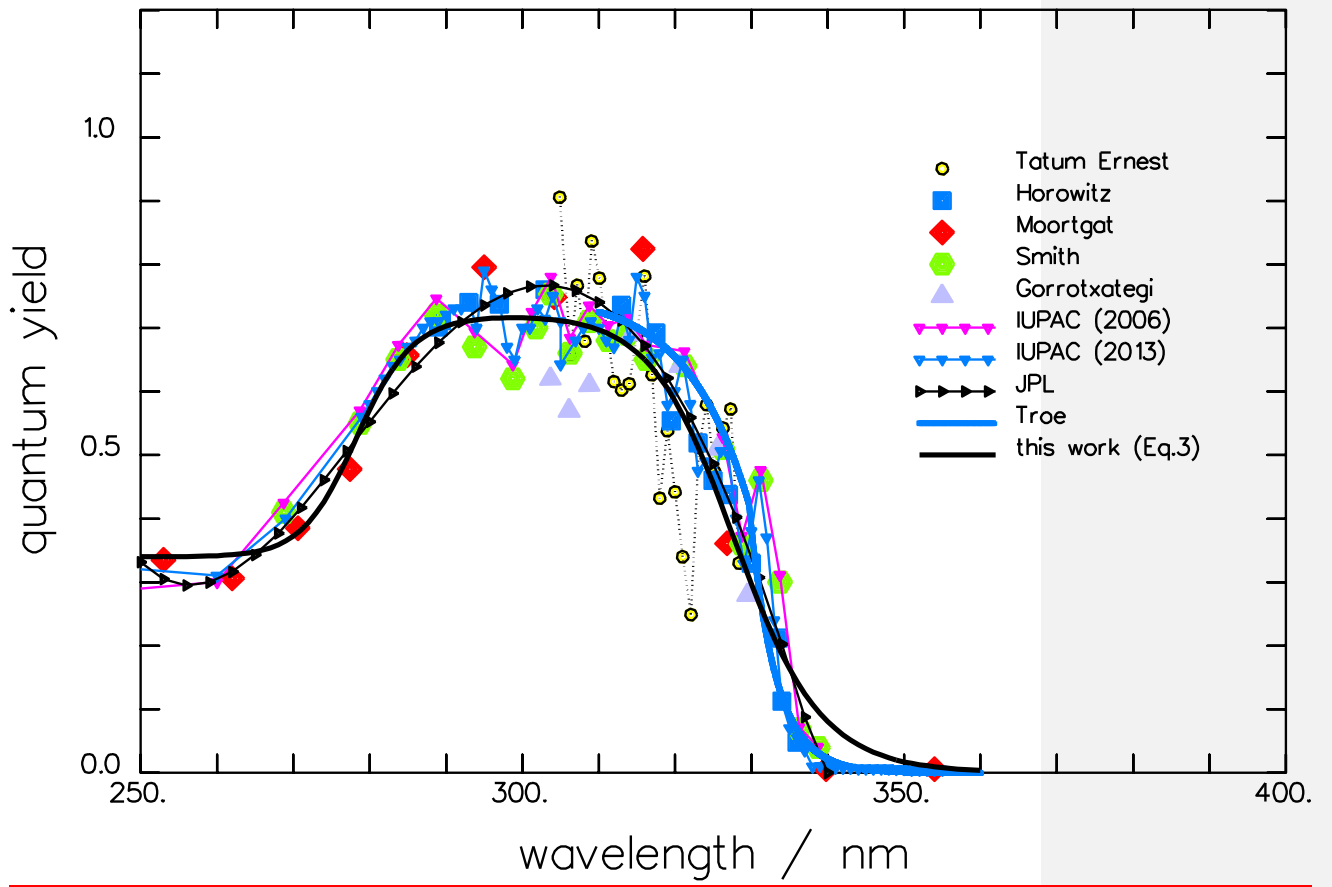
5
6
7

1
2
3
4
5

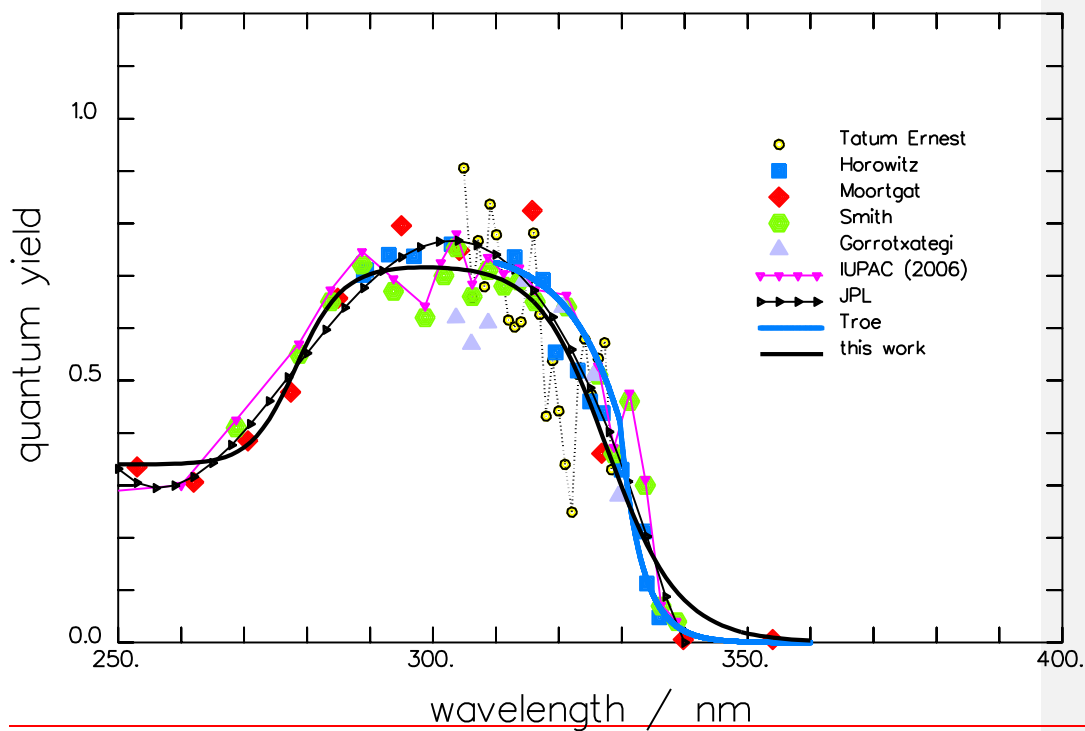
Table 5: Coefficients and 1σ errors of the equations in Table 4, along with the coefficients of determination e for the quantum yield functions. These parameters result from a global fit of all data, as described in Section 5.

	coefficient	value	error
	A_t	0.74	± 0.01
Φ_{rad} $e=0.904$	$\lambda_{0,t}$	327.4 nm	± 0.5 nm
	b_t	$5.4 \times 10^{-5} \text{ nm}^{-1}$	$\pm 0.5 \times 10^{-5} \text{ nm}^{-1}$
	A_s	0.40	± 0.04
	$\lambda_{0,s}$	279.0 nm	± 1.3 nm
	b_s	$5.2 \times 10^{-5} \text{ nm}^{-1}$	$\pm 2.4 \times 10^{-5} \text{ nm}^{-1}$
	A_t	1.0	fixed
Φ_{tot} $e=0.951$	$\lambda_{0,t}$	346.9 nm	± 0.5 nm
	b_t	$5.4 \times 10^{-5} \text{ nm}^{-1}$	$\pm 0.3 \times 10^{-5} \text{ nm}^{-1}$
	A_s	0.22	± 0.02
	$\lambda_{0,s}$	279.0 nm	± 1.3 nm
	b_s	$5.2 \times 10^{-5} \text{ nm}^{-1}$	$\pm 2.4 \times 10^{-5} \text{ nm}^{-1}$
	A_t	1.0	fixed
Φ_{mol} $e=0.934$	$\lambda_{0,t}$	346.9 nm	± 0.5 nm
	b_t	$5.4 \times 10^{-5} \text{ nm}^{-1}$	$\pm 0.3 \times 10^{-5} \text{ nm}^{-1}$
	A_m	0.74	± 0.01
	$\lambda_{0,m}$	327.4 nm	± 0.5 nm
	b_m	$5.4 \times 10^{-5} \text{ nm}^{-1}$	$\pm 0.5 \times 10^{-5} \text{ nm}^{-1}$
	A_s	0.18	± 0.02
	$\lambda_{0,s}$	279.0 nm	± 1.3 nm
	b_s	$5.2 \times 10^{-5} \text{ nm}^{-1}$	$\pm 2.4 \times 10^{-5} \text{ nm}^{-1}$

6



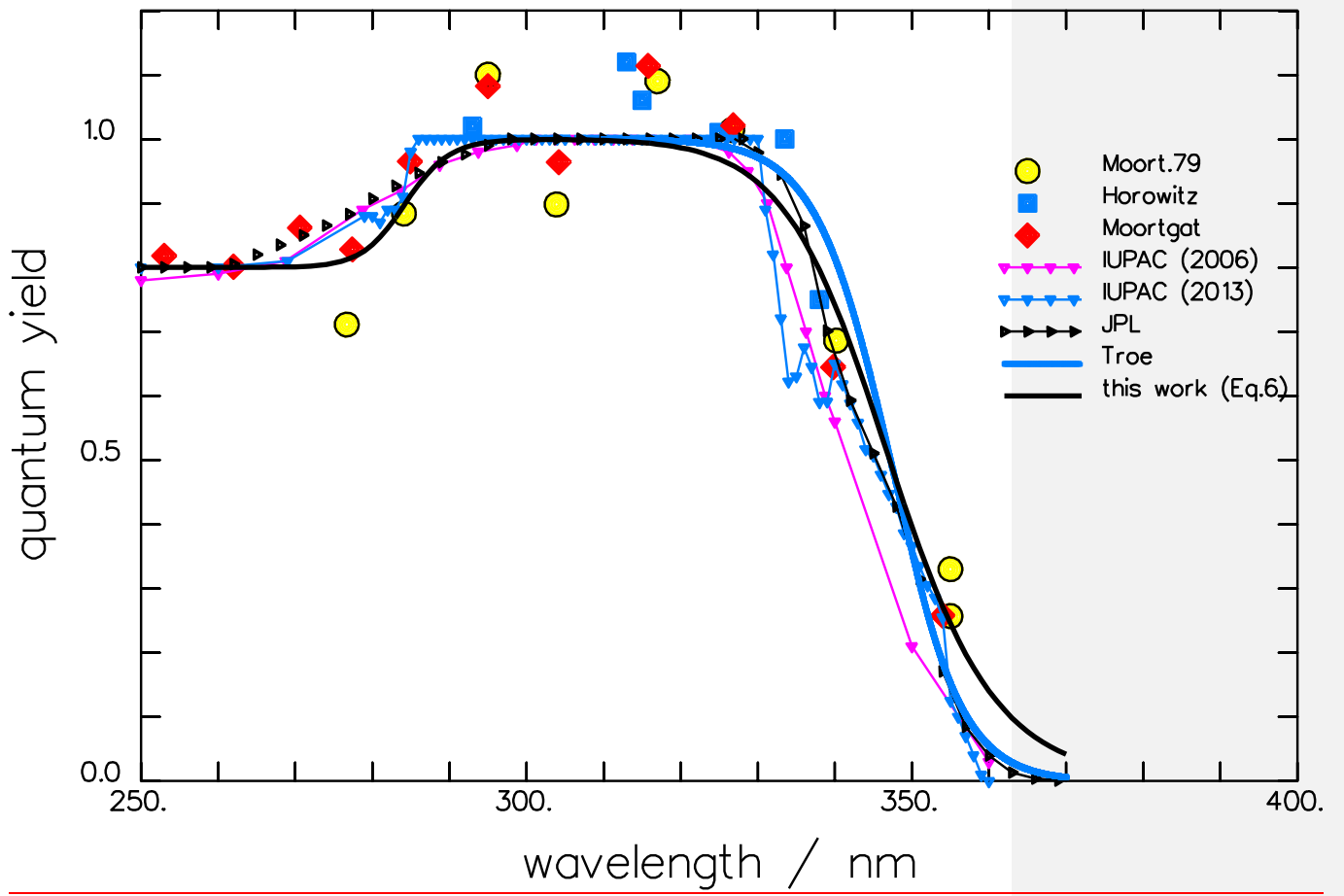
1



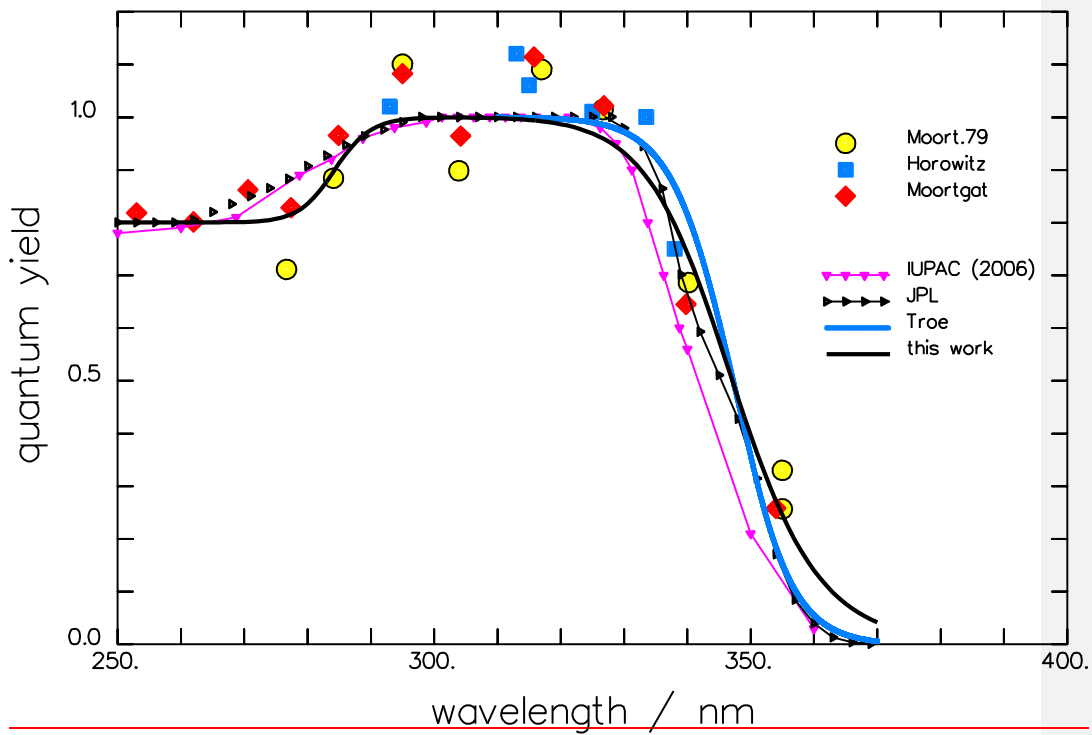
1
2
3
4
5
6
7
8
9
10

Figure 1: Spectrum of the quantum yield of the radical channel of the CH_2O photolysis at room temperature. Measured data used for the fit are indicated by the large full symbols (**Horowitz** and Calvert, 1978; **Moortgat** et al., 1983; **Smith** et al., 2002; **Gorrotxategi** Carbajo et al., 2008). The present fit and the theoretical curve from **Troe** (2007) are given by full lines. Recommended data are represented by small symbols connected by a thin line: **JPL** (Sander et al., 2011); **IUPAC (2006)**, **and IUPAC (2013)**. The line structure observed by **Tatum Ernest** et al. (2012) is indicated by open circles and a dotted line.

Formatiert: Schriftart: Nicht Fett



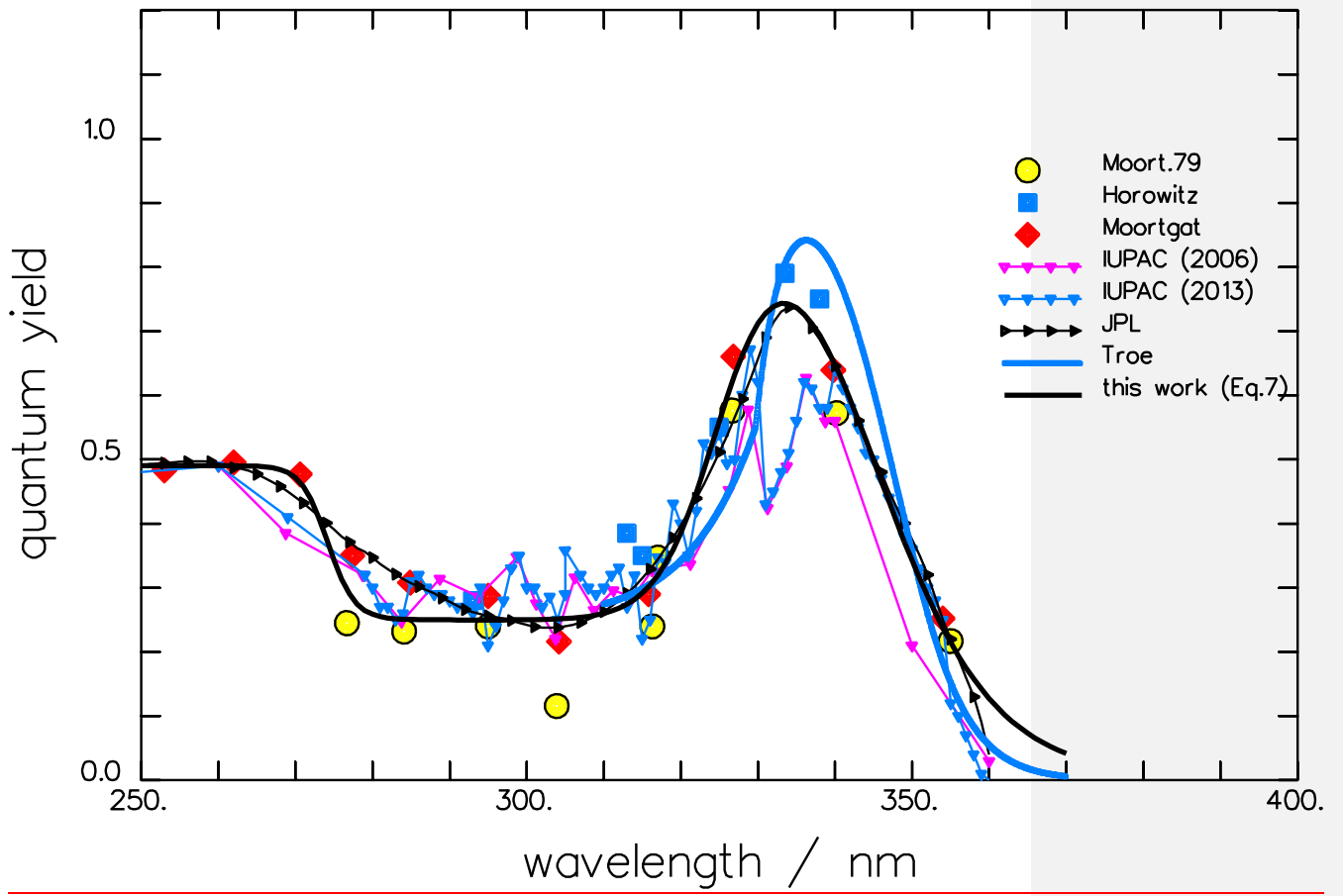
1



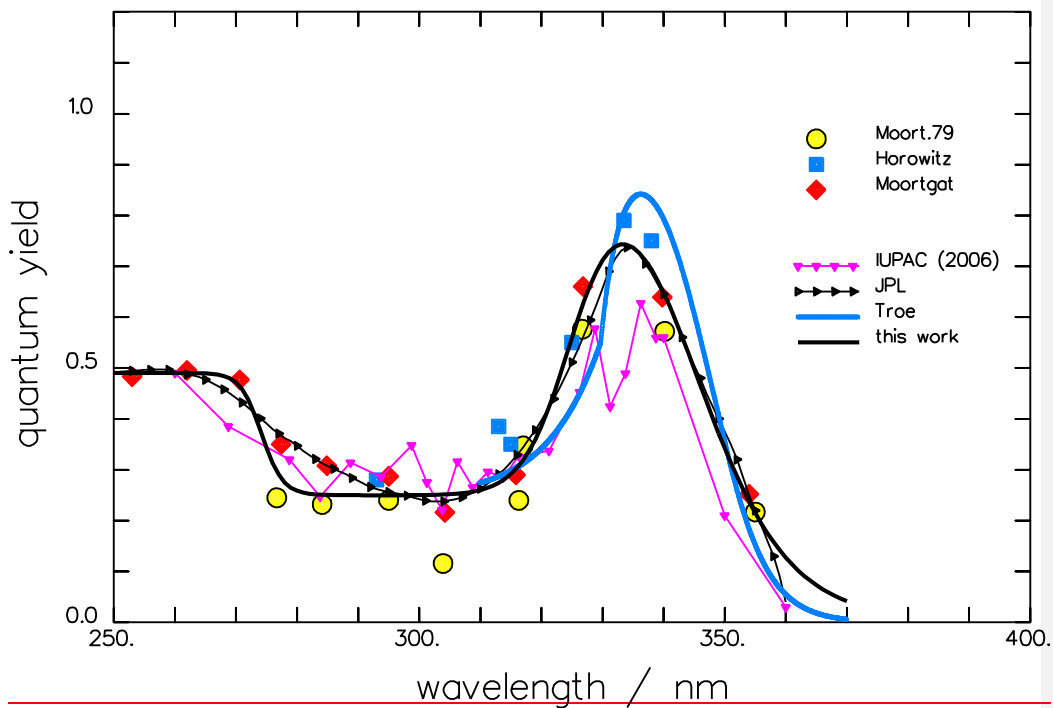
1
2
3
4
5
6
7
8
9
10

Figure 2: Spectrum of the quantum yield of the total CH₂O photolysis at room temperature. Measured data used for the fit are indicated by the large full symbols (**Moort.79:** Moortgat and Warneck, 1979, **Horowitz** and Calvert, 1978; **Moortgat** et al., 1983). The present fit and the theoretical curve from **Troe** (2007) are given by full lines. Recommended data are represented by small symbols connected by a thin line: **JPL** (Sander et al., 2011); **IUPAC (2006)**, **and IPUAC (2013)**.

Formatiert: Schriftart: Nicht Fett

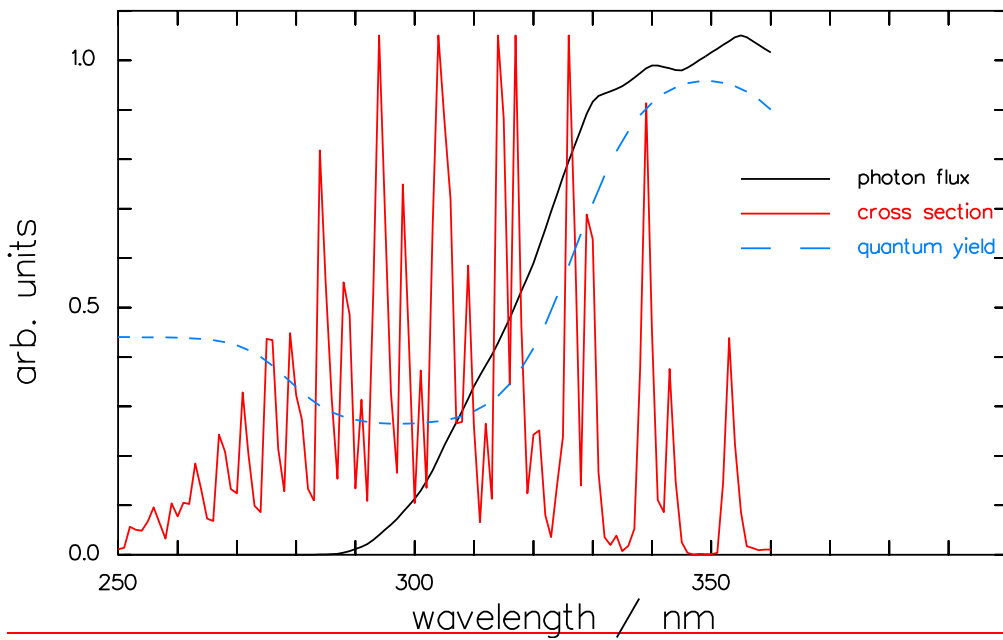
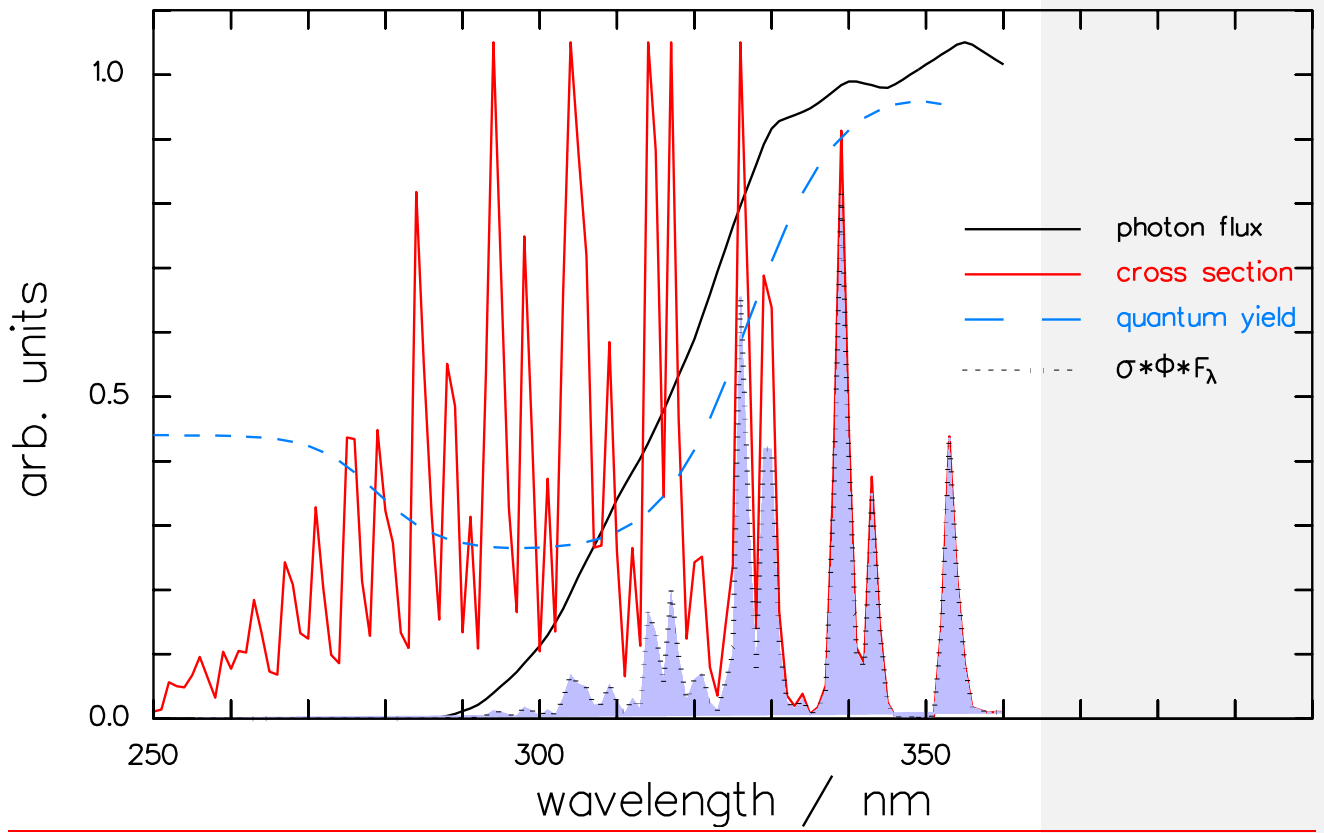


1



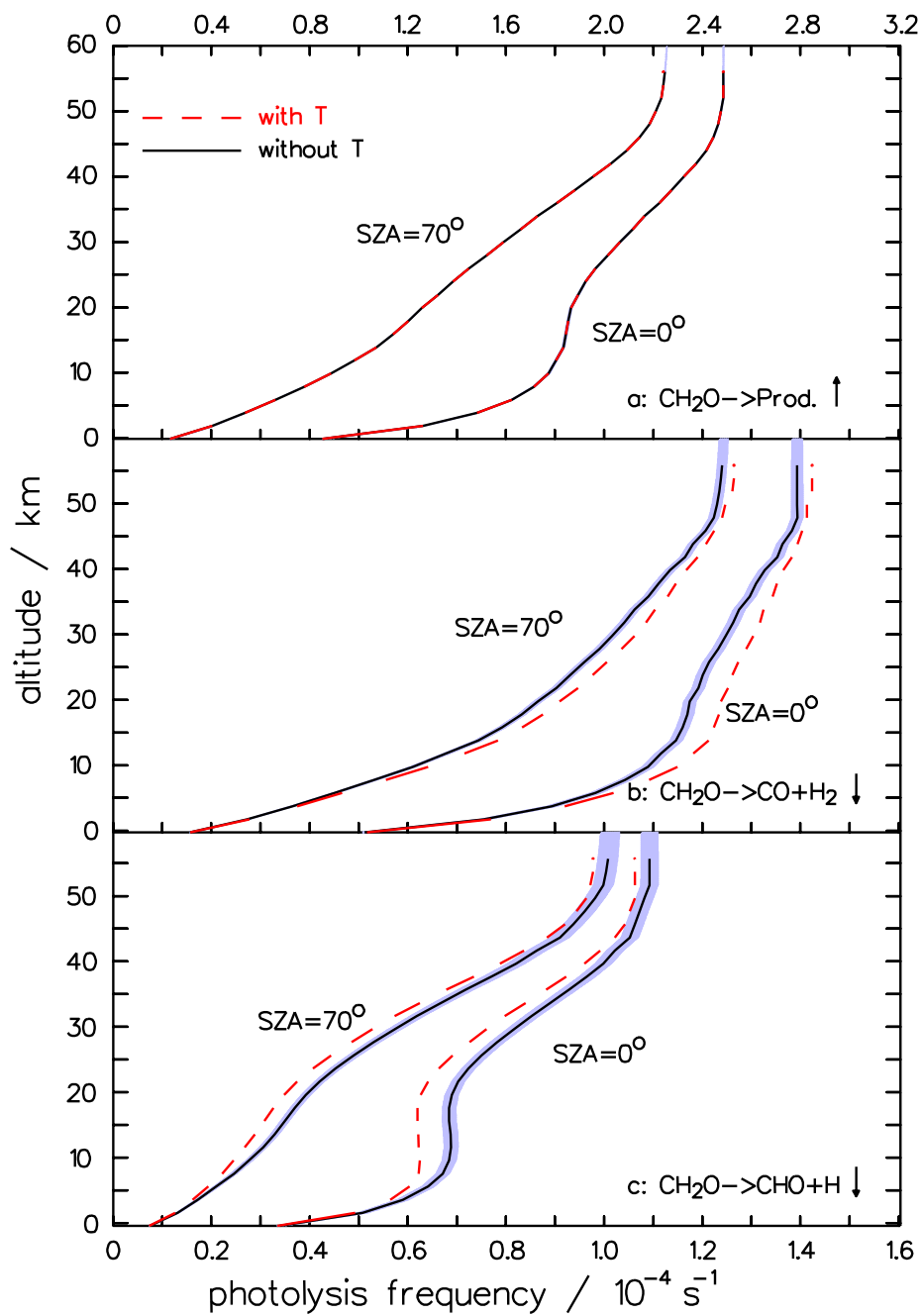
1
2
3
4
5
6
7
8
9
10

Figure 3: Spectrum of the quantum yield of the molecular branch of the CH₂O photolysis at room temperature. Measured data used for the fit are indicated by the large full symbols (**Moort.79**: Moortgat and Warneck, 1979, **Horowitz** and Calvert, 1978; **Moortgat** et al., 1983). The present fit and the theoretical curve from **Troe** (2007) are given by full lines. Recommended data are represented by small symbols connected by a thin line: **JPL** (Sander et al., 2011); **IUPAC (2006)**, and **IUPAC (2013)**.



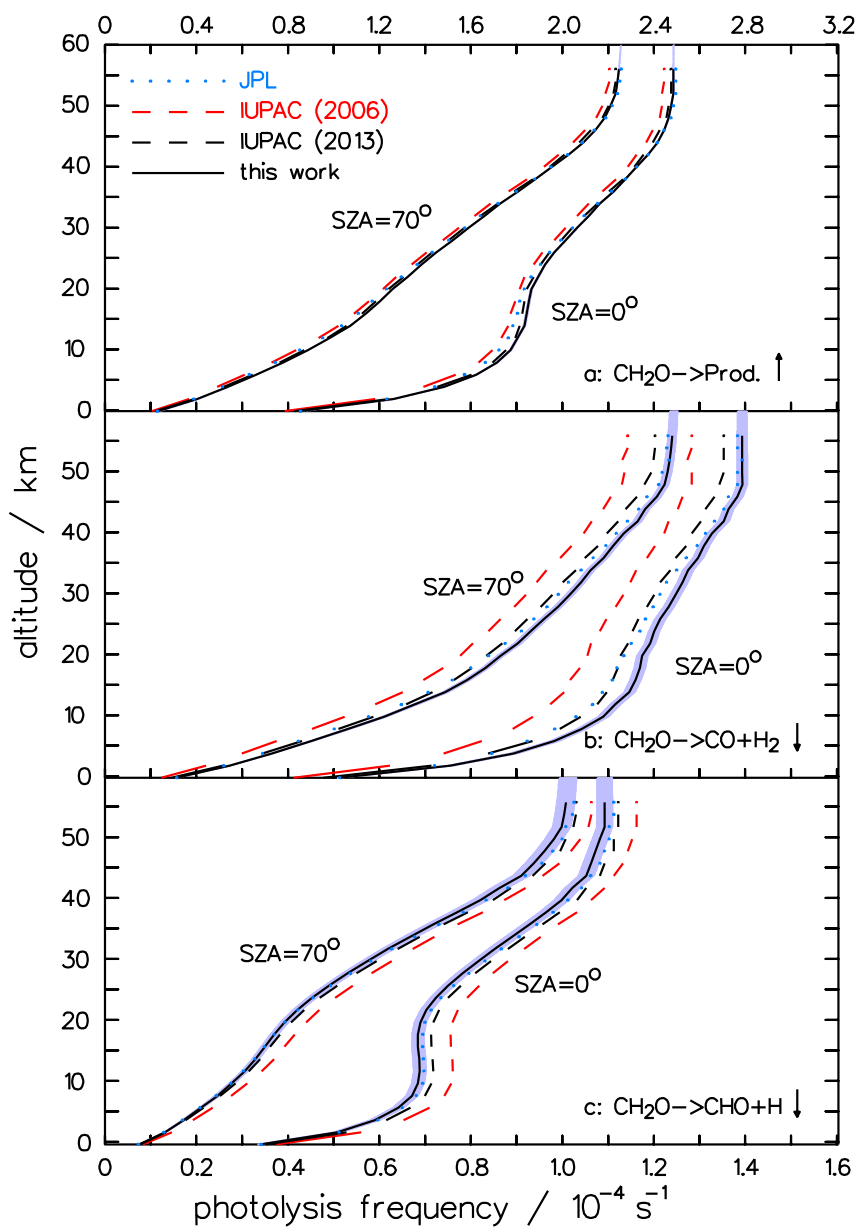
3

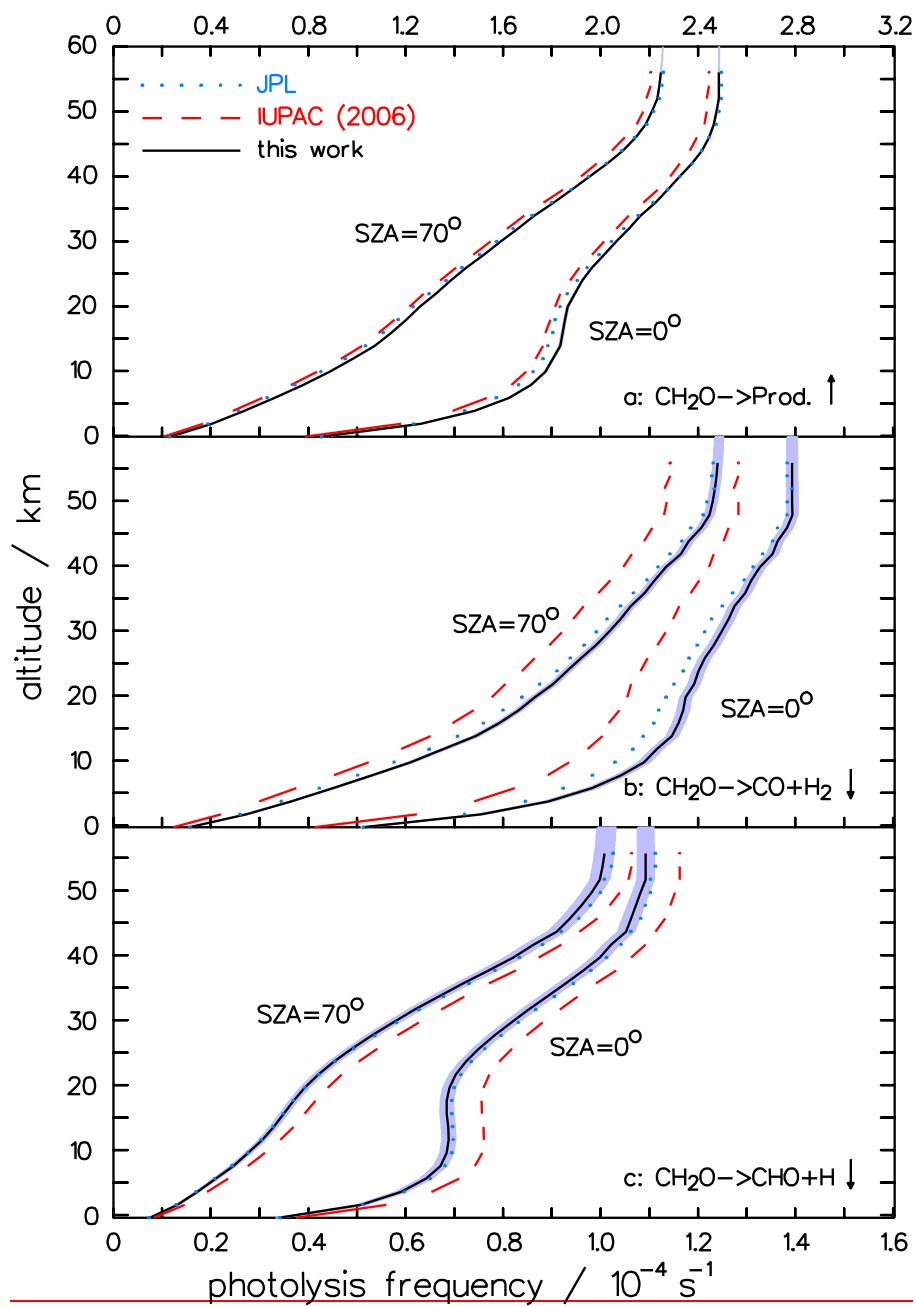
1 **Figure 4:** Spectra of the actinic photon flux density (WMO, 1985), the optical absorption
 2 cross section (Gratignan et al., 2007) and Φ_{mol} at 30 km altitude, 33° solar zenith angle, 227 K.
 3 The shaded area represents the integrand $\sigma \cdot \Phi \cdot F_{\lambda}$ of Eq.(11).
 4
 5
 6



7

1 **Figure 5:** Impact of a temperature dependent quantum yield, Φ_{rad} , on the altitudinal profile of
 2 the photolysis of formaldehyde: total photolysis (a), molecular channel (b), and radical
 3 channel (c). The dashed line indicates the impact of the temperature dependence of Φ_{rad} given
 4 by Troe (2007). The shaded areas mark the 1σ error bounds of the profiles based on the errors
 5 of the fitting parameters for the present quantum yields. The frequencies are depicted for two
 6 solar zenith angles (SZA). (The arrows point to the related ordinate)





1
 2 **Figure 6:** Comparison of the altitudinal profiles of the photolysis frequencies of
 3 formaldehyde from **JPL** (Sander et al., 2011); **IUPAC (2006)**, **IUPAC (2013)**, and the
 4 present work: total photolysis (a), molecular channel (b), and radical channel (c). The
 5 frequencies are depicted for two solar zenith angles (SZA). The shaded areas mark the 1σ
 6 error bounds of the profiles based on the errors of the fitting parameters for the present
 7 quantum yields. (The arrows point to the related ordinate)